This is a repository copy of *Crystallinity studies of PEKK and carbon fibre/PEKK composites: a review*.

White Rose Research Online URL for this paper:
https://eprints.whiterose.ac.uk/210437/

Version: Accepted Version

Crystallinity studies of PEKK and carbon fibre/PEKK composites: A review

Manuscript for *Composites Part B*

H. Pérez-Martín[1], P. Mackenzie[2], A. Baidak[2], C. M. Ó Brádaigh[1], D. Ray[1]*

[1] Institute for Materials and Processes, The University of Edinburgh, Edinburgh, United Kingdom
[2] Hexcel Composites Ltd., Duxford, Cambridge, United Kingdom

*To whom correspondence should be addressed: E-mail: Dipa.Roy@ed.ac.uk
Postal address:
1.140 Sanderson Building
King's Buildings
Edinburgh EH9 3FB
Scotland, UK

Abstract

Poly(etherketoneketone) (PEKK) is a thermoplastic, part of the poly(aryletherketone) (PAEK) family of polymers, with excellent mechanical performance and chemical resistance properties that make it an interesting candidate as a matrix for high-performance composites. Developing a thorough understanding of material properties is paramount in high-performance applications, and in the case of thermoplastics, crystallinity plays an essential role. This review paper covers the crystallisation morphology and structure of PEKK and CF/PEKK composites, crystallisation behaviour and kinetics under isothermal and dynamic conditions, and how these vary across different grades of PEKK with different terephthalic/isophthalic ratios. In the case of CF/PEKK composites, the impact of transcrystallinity development at the fibre-matrix interface, as well as the impact of carbon fibre inclusions on the crystallisation kinetics are discussed. Several crystallisation kinetics and transcrystallinity models available in literature are presented and discussed. The current limitations and future directions of CF/PEKK composites is also considered, covering manufacturing techniques such as autoclaves, automated tape placement, and 3D printing. This article draws comparisons to the better researched and established poly(etheretherketone) (PEEK) whenever relevant, in order to compliment the discussions on PEKK and CF/PEKK wherever literature is sparse.

Keywords

A. Polymer-matrix composites (PMCs); A. Thermoplastic resin; B. Fibre-matrix bond; B. Microstructures. Additional keyword: Poly(etherketoneketone) PEKK.

Contents

1. Introduction

Poly(aryletherketone)s (PAEKs) are a family of thermoplastics, widely used as a matrix in carbon fibre (CF) reinforced composites as structural materials in aeronautics, in parts like wing structures such as flaps, access panels and floor panels, amongst others [1–5]. These have excellent properties such as good impact, chemical and oxidation resistance, high-temperature performance and low density that make them apt for the role; and also possess an extended shelf life without refrigeration, are recyclable and possess a high repair potential, an advantageous quality that thermoset matrices do not possess [2,3,5–8]. The absence of a curing reaction also leads to potentially shorter processing times, enabling the combination and tailoring of different features and materials to suit the requirements of any particular application [7]. However, difficulties arise with regards to fibre impregnation due to higher viscosity, leading to a poor fibre-matrix interface, porosity and partial impregnation during production. In addition, achieving the desired level of crystallinity is critical in high-performance applications to attain the optimum combination of strength and toughness, requiring controlled processing conditions with optimum thermal cycles.

PAEKs differ from each other in the ether/ketone ratio they possess, as is described in Section 2.1 below. Poly(etheretherketone) (PEEK) has been widely studied over the last 30 years, with the focus on the processing of PEEK-based composites increasing in the past decade [1,9–15]. Poly(etherketoneketone) (PEKK), on the other hand, has been investigated much less extensively, arousing interest as a matrix for composite structural parts only in the recent years [2,5,7,10,16–19]. Its excellent mechanical properties and lower processing temperature than PEEK make it an interesting candidate for high-performance applications as well, leading to the development of new PEKK grades and matrix ranges in industry.

A different terephthalic/isophthalic content (T/I ratio) in PEKK result varying crystallisation kinetics and capabilities: a higher T/I ratio will require higher processing temperatures as a consequence of their melting temperature and viscosity, but have faster crystallisation kinetics than PEKK with a lower T/I ratio [20]. High crystallinity is desirable for performance, now that this increases the material's strength, stiffness, toughness and chemical resistance. In the case of the better understood PEEK, its chain structure allows for fast crystallisation kinetics; for PEKK, however, the availability of different T/I ratios calls for a thorough understanding of the kinetics in each case, to be able to optimise manufacturing. Furthermore, understanding the kinetics of the material in composite form is also of high importance, now that polymers have been observed to possess different crystallisation kinetics in presence of fibres [19,21,22].

This paper provides an analysis of PEKK's crystallisation morphology and kinetics, factors affecting this, and how the inclusion of carbon fibres impacts these behaviours. This is followed by an overview of the most relevant models used for the crystallisation kinetics of neat and composite PEKK, as well as an overview of some relevant transcrystallinity simulations. It is important to develop an understanding of unreinforced PEKK before considering its behaviour as part of a composite material, and therefore this paper offers a review of unreinforced PEKK wherever possible prior to any discussion of CF/PEKK composites. In addition, due to the limited literature on PEKK, a comparison is drawn from the more extensive literature available for PEEK and CF/PEEK whenever it is relevant.
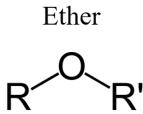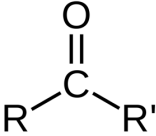
2. Crystallisation Morphology and Structure

The properties of PEKK, as well as that of any other PAEK, are a direct result of the molecular weight, polymer backbone, molecular organisation upon solidification, and any morphological changes that occur during subsequent thermal exposure [6]. The mode in which the polymers are crystallised also impacts the morphology, affecting the thermal stability of the resultant semicrystalline structure. This section will cover the differences in the structure of PAEKs and the various grades of PEKK, the morphology of crystallised PEKK at molecular and micron level, and will discuss how crystal nucleation and growth is impacted by the inclusions of carbon fibres, potentially resulting in a transcrystalline phase at the fibre-matrix interface.

2.1. Chain Morphology

The backbone of all PAEK polymers consists of aromatic rings connected by ether or ketone linkages, the order of which gives the name to the specific polymer as shown in Table 1. The stiffness that aromatic rings bring to the backbone chain, combined with a high chain linearity and little to no branching [6,10] results in tough, strong thermoplastics suitable for high-performance composite applications. Ketone linkages are also stiffer than ether linkages, which gives rise to PEKK being the stiffest of the four polymers shown in Table 1.

Table 1: Polymer repeat units for PEEK, poly(etherketone) (PEK), poly(etherketoneetherketoneketone) (PEKEKK) and PEKK. Drawn after [10].

	Structure	Name	Ketone (%)
Ether $R{-}O{-}R'$		PEEK	33
		PEK	50
Ketone $R{-}C({=}O){-}R'$		PEKEKK	60
		PEKK	67

In some thermoplastics from the PAEK family, material properties can be further modified by controlling the inclusion of different isomers during synthesis. In the case of PEKK, this is created by combining diphenyl ether (DPE) with terephthalic acid (T) or isophthalic acid (I). These result in the creation of para- and meta- isomers respectively as per Figure 1. Different content of these linkages result in different grades in PEKK, and these are often classified with a T/I ratio (terephthalic/isophthalic content). A low T/I ratio entails a higher content of meta- linkages, resulting in more flexible chains and decreasing the melting temperature [5,10]. This facilitates composite manufacturing, but at the cost of achieved crystallinity as a consequence of the lower linearity of meta-linkage, which causes disruption of the crystal packing [17].
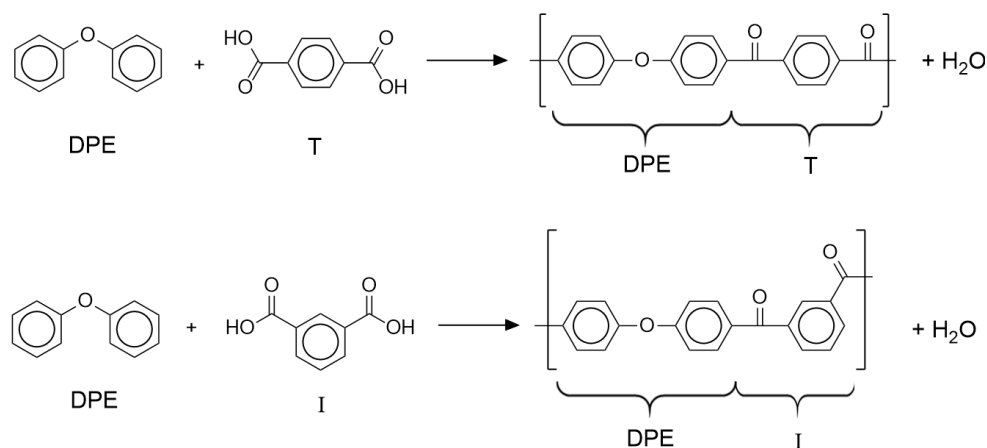
Figure 1: Chemical reaction for production of 1,4- (top) and 1,3- (bottom) substituted PEKK, by combining diphenyl ether (DPE) with terephthalic acid (T) or isophthalic acid (I).

In the case of PEEK, there is no way of achieving these differences in grades by varying para/meta linkages. The polymer is often produced by reacting 4, 4' difluorobenzophenone, hydroquinone and potassium carbonate, as per Figure 2 [23]. A lower ketone content makes PAEK polymers more malleable, allowing PEEK to crystallise more readily than PEKK.
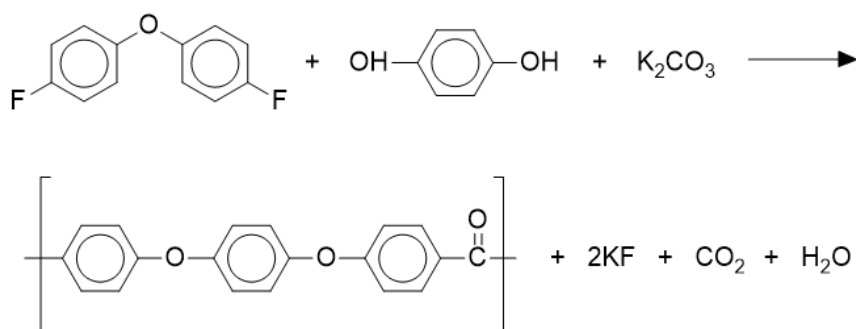
Figure 2: Chemical reaction for prodution of PEEK by combining 4, 4' difluorobenzophenone, hydroquinone and potassium carbonate. Drawn after [23].

Overall, the PAEK family of polymers crystallise easily due to the ether and ketone linkages they contain [23]: while the aromatic rings present in the backbone chain bring a lot of rigidity to the material, the flexible ether linkages, provide some flexibility and allow for processability. The ketone linkages, despite being stiffer than ether linkages, remain quite compact, which along with both functional groups sharing essentially the same angle formation, allow for neighbouring molecules to pack together without necessarily having identical sequencing. This is key in the potential for crystallisation. In the case of PEEK, as this is a highly even polymer with no meta- phenyl links, chain packing is more readily achievable. The higher ketone content in PEKK results in a heavier, stiffer chain structure and generally a more viscous polymer with slower crystallisation kinetics. Crystallisation is also dependent on the T/I ratio, therefore making PEKK a more tuneable but challenging material to optimise [5,17,24]. This is conveyed in Figure 3, which shows a comparison of the chain packing of PEEK and of different T/I ratios of PEKK when sequencing is not identical.

5

Figure 3: Chemical structures and chain packing of (a) PEEK and PEKK with various T/I ratios: (b) 100/0, (c) 50/50, (d) 0/100.

Table 2 below shows different grades of KEPSTAN® PEKK offered by Arkema, where both the T/I ratio and the viscosity are varied [25]. An increase in the melt volume index within a specific T/I ratio as denoted in the second row suggests a lower viscosity.
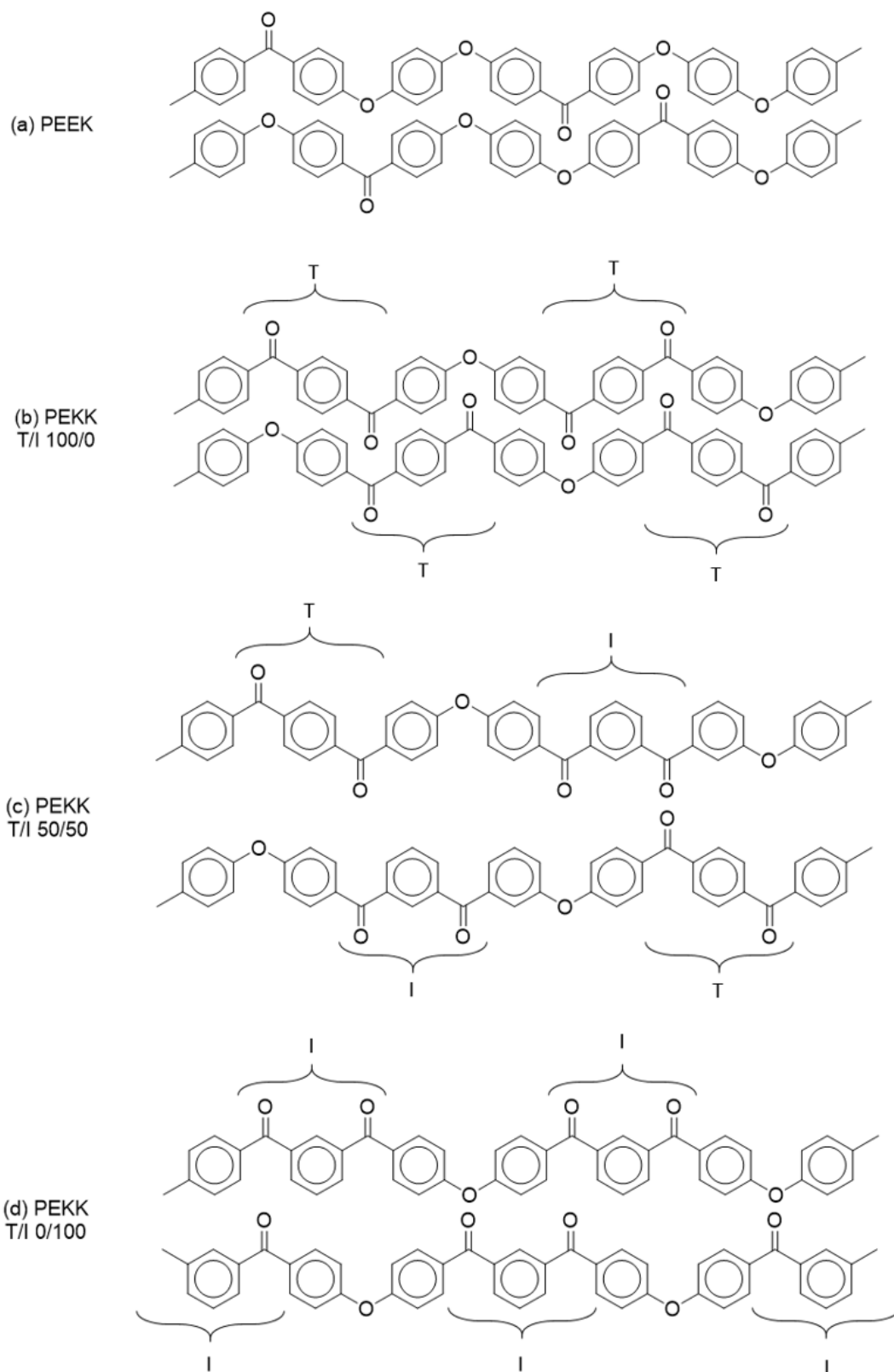
Table 2: KEPSTAN(R) PEKK commercial range grades, based on T/I ratio and viscosity (adapted from webinar presentation) [25].

Viscosity level	1	2	3	4
Melt Volume Index*	11-24**	4-8	8-16	16-25
6000 series (T/I 60/40)	6001	6002	6003	6004
7000 series (T/I 70/30)	7001	7002	7003	7004
8000 series (T/I 80/20)	8001	8002	8003	8004
* MVI in cc per 10', at 380°c and under 1kg				
** MVI measured under 5 kg for level 1 viscosity				

2.2.   Unit Cell Structure

All polymers contain an amorphous fraction of material due to polydispersity, material "defects" such as chain ends, and the interlinked nature of crystallisable segments preventing full crystallisation [6]. As described previously, the higher ketone content in PEKK results in higher chain stiffness, adding to the crystallisation difficulty. Nonetheless, PEKK can be crystallised during the manufacturing process or with subsequent annealing. Depending on the crystallisation conditions (from the melt, cold or solvent), not only one but two unit cell forms of crystallised PEKK may be present [10,11,18]. Unit cells are the simplest repeating unit within a crystal form, and are the building blocks of the spherulitic structures that form in PEKK. Spherulite formation is discussed further in Section 2.3.

These two different unit cell forms have been identified by Gardner et al. [17] as follows, and can be observed in Figure 4 and Figure 5 (form 1 and form 2 (i)). In the words of the authors in one of their articles [10]:

> *"Form 1 has a two-chain orthorhombic unit cell with chains located at the corner and centre of the unit cell and is characterised by edge-to-face phenyl interaction. In contrast, form 2 has been assigned a one-chain (metrically) orthorhombic unit cell with face-to-face phenyl interactions [17]. (An alternative unit cell has been proposed by Blundell and Newton, and this also has face-to-face phenyl interactions [26].) The two polymorphs have different melting temperatures, and, in some cases, the form 2 structure is capable of converting into form 1 after melting."*

As mentioned, an alternative form 2 unit cell was identified by Blundell and Newton [26], with a 2-chain orthorhombic structure and face-to-face phenyl interactions, shown in Figure 4 (form 2 (ii)) [8,18,26,27]. There is no dual unit cell form in the case of PEEK due to its higher ether content, and so only crystallises as form 1 [26].
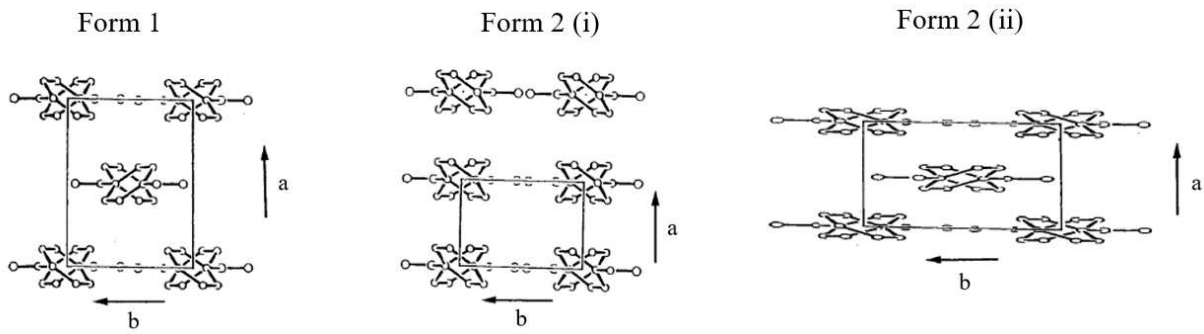
Figure 4: Crystal packing models of PEKK of form 1 (two-chain orthorhombic); form 2 (i) (one-chain orthorhombic as per Gardner et al. [17]); and form 2 (ii) (two-chain orthorhombic as per Blundell and Newton [26]) and unit cell dimensions.

Based on Figure 4, a three-dimensional schematic of each unit cell is included in Figure 5. The dimensions of each unit cell are available in Table 3.
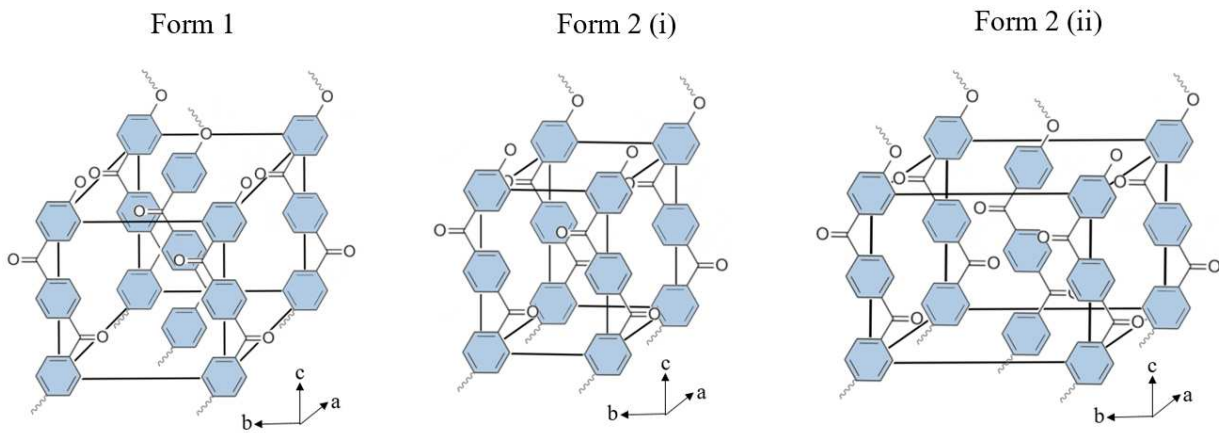
Figure 5: 3D schematic of crystal packing models of PEKK, based on Figure 4.

Table 3: Dimensions for the different unit cell forms of PEKK.

Unit cell	Dimensions (nm)			Reference
	a	b	c	
Form 1	0.769	0.606	1.016	[17]
	0.767	0.606	1.008	[27]
Form 2 (i)	0.393	0.575	1.016	[17]
Form 2 (ii)	0.417	1.134	1.008	[26,27]

This polymorphism has also been reported in other PAEKs. The presence of forms 1 and 2 has been found to depend on two factors:

a) Crystallisation mode, with melt crystallisation favouring form 1; and cold or solvent crystallisation favouring mode 2 [8,10,18,27].
b) Chain stiffness, which increases in PAEKs with higher ketone content and with a higher T/I ratio, and favours form 2 [8,10,26].

In the case of PEKK, Gardner et al. [10] summarised the impact of T/I ratio and crystallisation method in the "phase diagram" shown in Figure 6. Further details on the impact of these variables can be found in their work, as well as in [8,17,18,26,27].
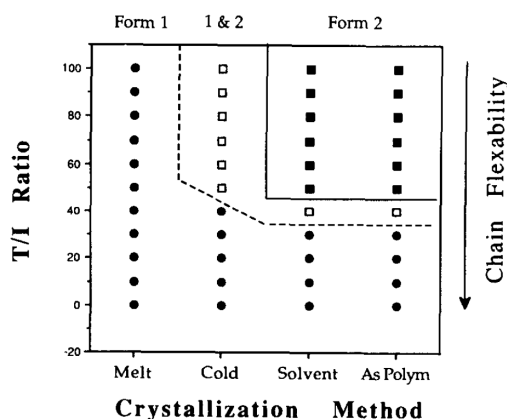
Figure 6: "Phase diagram" showing the occurrence of the two crystalline polymorphisms in PEKK as a function of the T/I ratio and the crystallisation conditions [10].

2.3. Spherulitic Growth and Lamellar Structure

Regardless of the unit cell form that PEKK chains organise into when crystallising, these unit cells begin to form upon nucleation as shown in Figure 7 and Figure 8. Nucleation takes place when polymer chains become arranged in a unit cell form. This then allows PEKK chains to further arrange themselves to form individual lamellae, as per Figure 9. These are separated by an amorphous zone consisting of chain ends and entangled segments. Lamellae then develop into sheaf-like structures which grow further in and out of plane to form spherulites, as shown in Figure 10 [1,11,23,28]. Choupin et al. [2] observed the spherulitic growth of PEKK 60/40 with hot stage microscopy, shown in Figure 11. The crystalline entities can be observed to grow independently with the same size until impingement, typical of instantaneous nucleation.
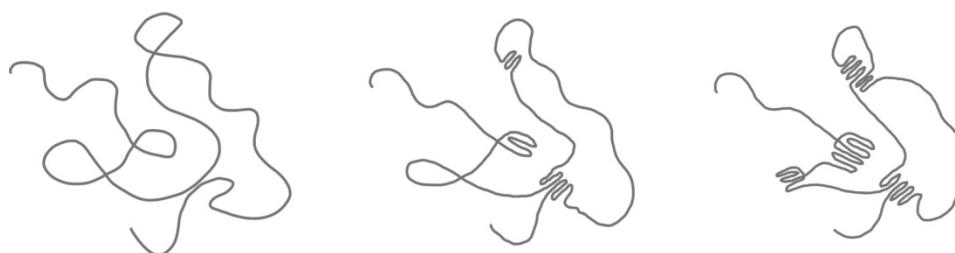
Figure 7: A schematic showing homogeneous nucleation, where a polymer chain commences nucleation without the presence of a foreign phase or particle.
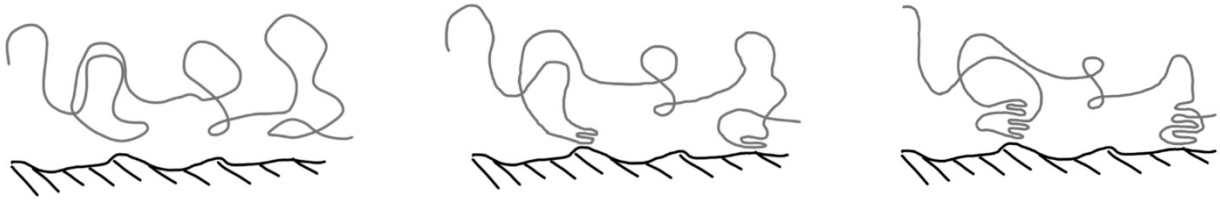
Figure 8: A schematic showing of heterogeneous nucleation, where a polymer chain commences nucleation on the surface of a foreign particle.
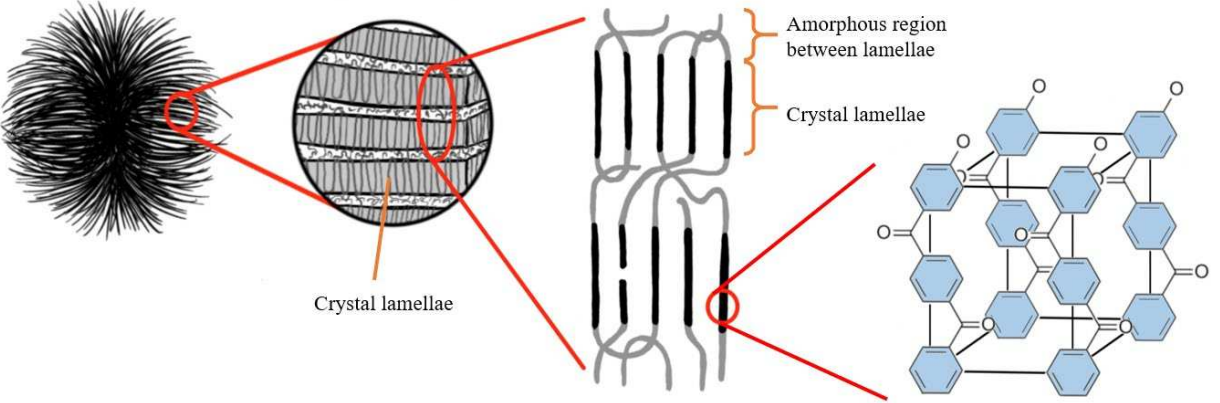
Figure 9: Crystalline morphology schematic, showing lamellae (crystal) and amorphous regions of a spherulite. Magnitude increases from left to right. Drawn after [11,28].
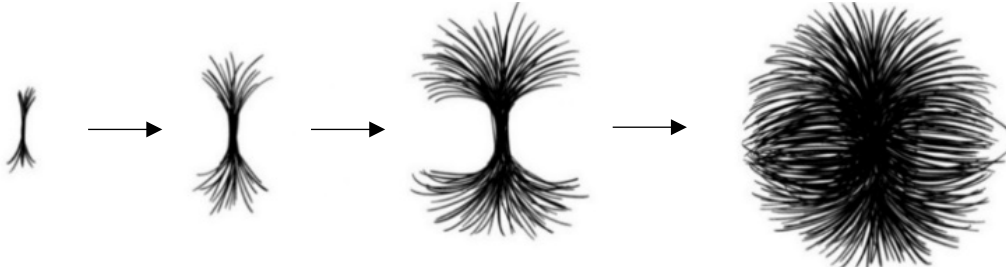
Figure 10: Spherulite formation schematic. Drawn after [28].
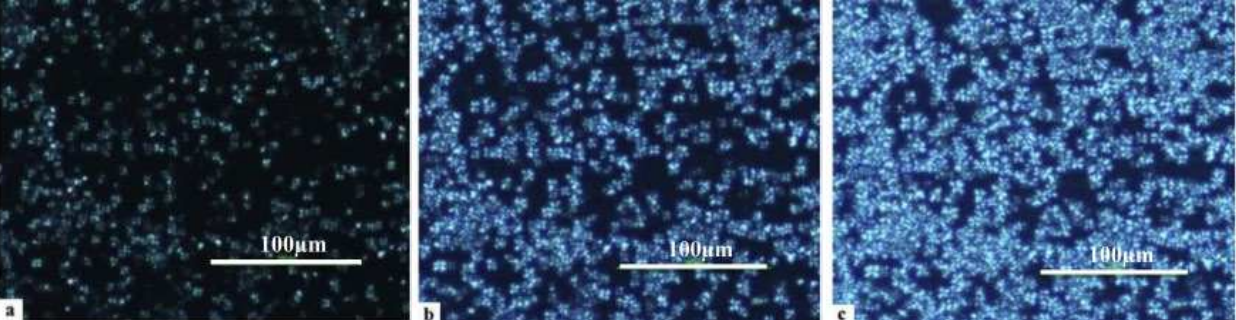
Figure 11: Micrographs of PEKK 60/40 crystallised from the melt at 270°C during (a) 20 min, (b) 30 min and (c) 40 min [2].

10

Spherulitic nucleation and growth are dependent on several factors. A low nucleation density and therefore large spherulites can be obtained if the polymer is held in the melt during extended periods of time, enough to destroy any pre-existing nucleation sites. The temperature can then be dropped to crystallise the material, in which spherulites will grow for as long as the material is held at crystallisation temperature, or until two spherulitic fronts meet and impinge on each other. Alternatively, higher nucleation densities can be obtained if the polymer is not held in the melt long enough, or if annealed, which may be common in high-paced manufacturing techniques. Lee and Porter [29] observed this phenomenon, where they held PEEK samples with carbon fibres at 390°C (in the melt) for different lengths of time, and cooled to 270°C at 0.5°C/min, followed by quenching to room temperature. The results can be observed in Figure 12 below.
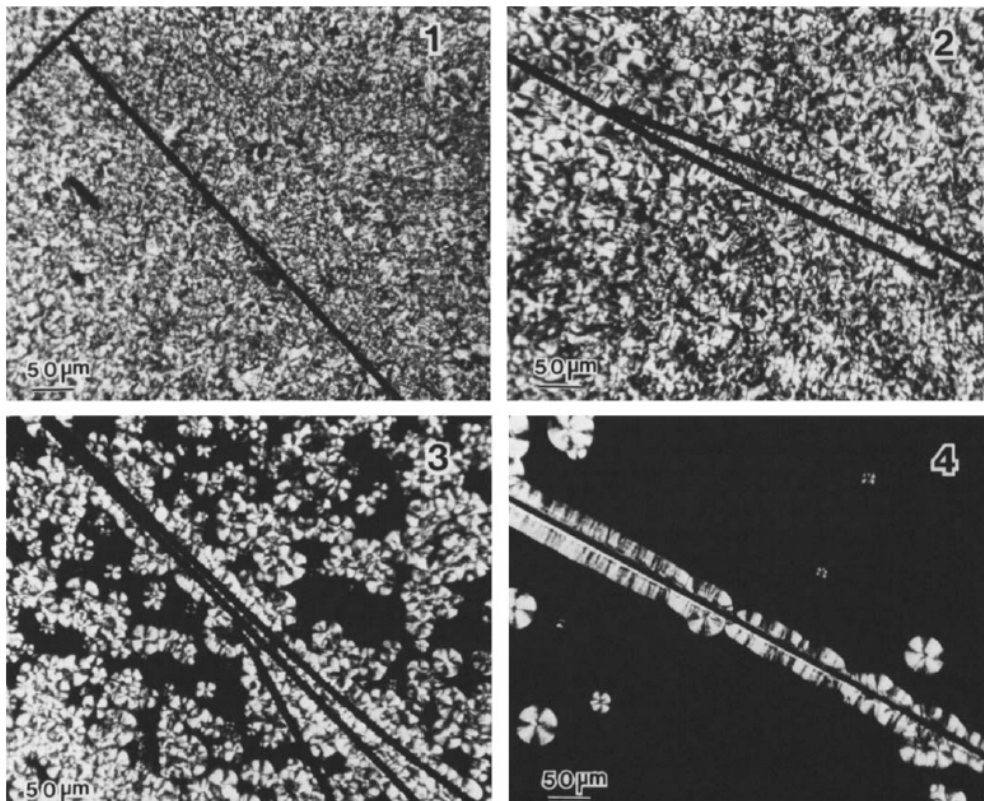
Figure 12: Optical micrographs of PEEK with carbon fibres: samples held at 390°C for (1) 0.5h; (2) 2h; (3) 3h; (4) 4h and cooled (0.5°C/min) to 270°C, followed by quenching to room temperature [29].

The matrix bulk in sample 4 (held for the longest time) can be observed to have fewer but larger spherulites, whereas the opposite happens with the shorter times, resulting in the impingement of small spherulites in sample 1. Nucleation on fibre surfaces as observed in Lee and Porter's findings [29] will be discussed in the following section.

Blundell et al. [1] also observed such high nucleation densities in the bulk of CF/PEEK samples when the material was melted at a temperature not high enough to melt the last traces of crystallinity. They melted a sample at 355°C for 10 minutes (15°C above the peak melting point in a DSC scan), followed by cooling at 10°C/min. This resulted in self-seeding of the crystallisation process, resulting in a very high nucleation density and preventing spherulitic growth by mutual impingement, and therefore sheaf-like structures were formed instead. This is in contrast to samples held in the melt at 400°C for 10

minutes and then cooled at 10°/min, where nucleation density was much lower and spherulite structures were clearly formed. SEM images of this can be found in their work [1].

2.4.   Carbon fibre/PEKK and Transcrystallinity

The use of fibres with high-performance thermoplastics has become increasingly popular in the aerospace and automotive industries, and is almost a necessity, due to their high strength and stiffness per unit weight. This makes composites an attractive replacement for previously used heavier materials for the same applications, such as steels, titanium and aluminium. The fibre/matrix interface plays an essential role in their performance, due to it being responsible for the transmission of stress from the matrix to the fibres. A transcrystalline interface has been observed in thermoplastic composites, the presence and size of which is dependent on the nucleating activity of the fibre surface as well as the crystallisation kinetics of the matrix [30].

In the case of carbon fibres, transcrystalline growth has often been related to the graphitic nature of the fibre surface, as well as the higher thermal conductivity promoting a conductivity mismatch between fibre and matrix [1,30]. In the case of CF/PEEK and CF/PEKK in particular, Hsiao et al. [19] concluded that, on top of these two factors, a similarity in unit cells is also a potential source of nucleation. The high nucleation density on the fibre surface causes neighbouring nuclei to impinge, resulting in a compact, unidirectional growth of crystals normal to the fibre surface, often referred to as "epitaxial" growth. This is in contrast to the spherulitic nature of crystallisation in the matrix bulk. [21,29–35]. A schematic applicable to the crystallisation of PEEK and PEKK is shown in Figure 13.
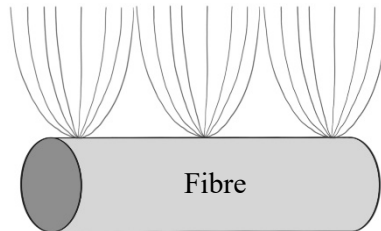
Figure 13: Diagram of transcrystalline interface growth on the fibre surface. Drawn after [30].

The presence of transcrystallinity on CF/PEEK and CF/PEKK composites is still a topic under investigation, as different observations have been reported by authors. Blundell et al. [1] observed no evidence of transcrystalline growth in etched CF/PEEK samples, but instead observed spherulitic growths on the fibre surface as per in the matrix bulk. On the other hand, Lustiger [36] observed differences in the transcrystallinity of CF/PEEK depending on the type of fibre used, something also noted by Chen and Hsiao [30] in CF/PEKK. The following paragraphs will investigate the source of these discrepancies.

In Lustiger's study [36], clear differences in the transcrystalline region were observed between low-modulus (AS4) and high-modulus (HMS) carbon fibres, where the surface energy played a critical role in the form of the transcrystalline region. The unsized fibres were placed in molten PEEK and held long enough in the melt to minimise any potential nucleation sites in the bulk, and to allow for large spherulitic growth. Flat-on lamellae were observed to grow on the AS4 fibres, whereas a high nucleation

density was observed on the HMS fibres, resulting in impingement before spherulites can fully form and therefore transcrystallinity. This is explained in terms of the fibres' surface energy: AS4 fibres have higher surface energy, inviting the amorphous interlamellar regions to interact with them, resulting in lamellae lying flat-on; whereas HMS fibres are relatively inert resulting in little attraction between the fibre surface and the amorphous polymer, and therefore lamellae can form perpendicular to the fibre surface. SEM micrographs displaying this behaviour are shown in Figure 14. These observations have been made in other literature [21,29,35–37] where it was concluded that the graphitic nature of HMS fibres results in a higher nucleation tendency, consistently generating transcrystallinity in PEEK and other semi-crystalline polymers. This is in line with the observations by Blundell et al. [1] mentioned earlier, as the carbon fibres used were AS4 (higher surface energy and therefore no transcrystallinity).
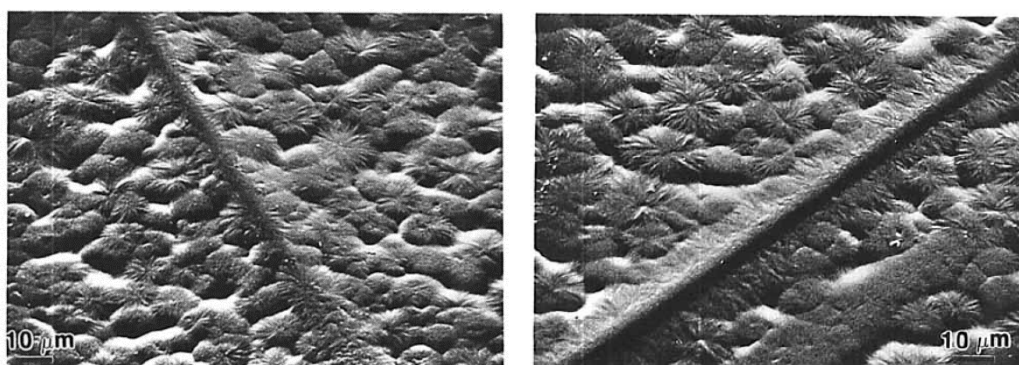
Figure 14: Left: spherulite nucleation in PEEK in contact with an unsized AS4 fibre
Right: transcrystallinity in PEEK in contact with unsized HMS fibre [36].

Chen and Hsiao [30], who studied transcrystallinity of PEEK and PEKK on different fibres, observed a transcrystalline interface on pitch-based carbon fibres, taking the characteristic epitaxial form; while this was not the case on PAN-based AU4 carbon fibres. Pitch-based carbon fibre has interactive edge planes which result in a topographical match with the matrix crystal structure, whereas PAN-based carbon fibre is mostly defect-free, hindering nucleation on the fibre surface.

Lee and Porter [29] studied the nucleation ability of PEEK on Thornel 300 carbon fibres (PAN-based) supplied by Union Carbide, which clearly developed a transcrystalline region, particularly when CF/PEEK samples were held in the melt for long times and few spherulites are seen in the bulk, as shown in Figure 12. It is unclear, however, where Thornel 300 fibres fall in comparison with the previously mentioned fibres with regards to their strength and modulus. In fact, a connection between pitch vs. PAN-based fibres, as well as high-strength vs. high-modulus, and their connection and influence to transcrystallinity, is not clearly outlined in literature, and would be interesting to investigate further.

Overall, it can be concluded that PEEK and PEKK have the capability to form transcrystalline interfaces in the presence of carbon fibres, as long as said fibre has the correct surface characteristics to do so. There is some uncertainty, however, regarding the presence of transcrystallinity and its influence on mechanical properties, as literature has reported contradictory conclusions. The fibre volume fraction (FVF) of CF/PEKK and CF/PEEK composites has been observed to have an effect on this interface phenomenon. A higher fibre content results in a lower matrix spacing between fibres, limiting crystallisation growth both in the bulk and on the fibres [21,30,31]. While Chen and Hsiao [30]

observed a 48% increase in force during microdebonding tests of a single AU-4 filament/PEKK composite with a transcrystalline region (compared to its transcrystallinity-free counterpart), an increase in FVF decreased this difference, reducing to 0% difference at a FVF of 60%. Waddon et al. [35] observed preferential fracture along the line where two transcrystalline growth fronts met in a CF/poly(etherketone) sample, which is most likely to occur in samples with high fibre content. This may be a reason for the reduced impact of transcrystallinity in higher FVF composites.

The development of a transcrystalline interface is also heavily reliant on the composites processing: melting and crystallisation temperatures, holding times and cooling rates. This, as well as its effects on mechanical properties, is elaborated on in Section 3.3, after presenting the crystallisation kinetics of unreinforced PEKK.

3. Crystallisation Kinetics

As discussed above, the properties of PEKK and any semi-crystalline thermoplastic polymer depend on the degree of crystallinity and their morphology. The understanding of crystallisation mechanisms is of fundamental importance in the case of high-performing thermoplastic materials, and plays a fundamental role in composite processing. This section will therefore provide a review of both isothermal and non-isothermal crystallisation kinetics of unreinforced PEKK, as well as the effect that carbon fibre reinforcement might have on these kinetics. A selection of graphs and data from various articles is included at the end of this section, showing the variation of matrix-dominated mechanical properties with respect to the manufacturing cycle the material undergoes. Studies covering the impact of thermal cycles on specifically crystallinity and mechanical behaviour are sparse, particularly on CF/PEKK. Thus, some data covering unreinforced PEKK, PEEK and CF/PEEK composites is included.

3.1. Isothermal Crystallisation

Quiroga Cortés et al. [5] assessed the effect of both holding temperature and holding time on the crystallisation of unreinforced PEKK 60/40 (PEKK KEPSTAN 6003, supplied by Arkema). The results of this are shown in Figure 15 and Figure 16. Two endotherms can be observed: the standard melting peak, referred to as the high temperature endotherm (HTE) at around 300°C, and a smaller peak, called the lower temperature endotherm (LTE) at approximately 10°C above the holding temperature.
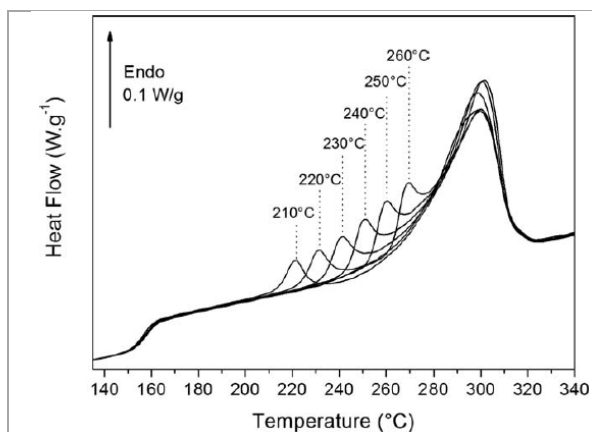
Figure 15: DSC thermograms of isothermally crystallised PEKK 60/40 at different temperatures (as indicated) for 60 min [5].
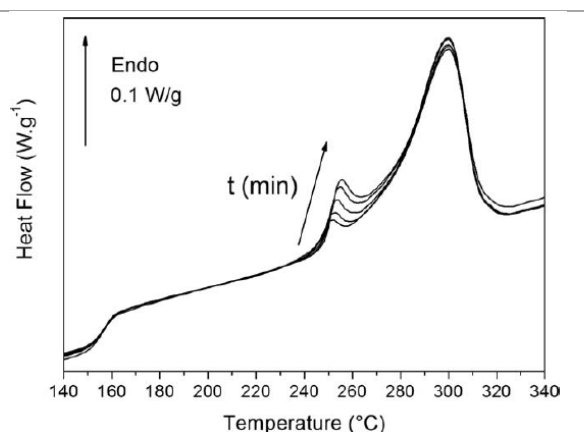
Figure 16: DSC thermograms of isothermally crystallised PEKK 60/40 at 245°C for different time periods [5].

Double melting behaviour has been observed by several authors in PEKK isothermal crystallisation [2,5,17,18,20,24,38], as well as in PEEK [11,39–52] during DSC. This additional low temperature endotherm (LTE) is reported to appear 10-20°C above the isothermal crystallisation temperature to which the polymer is subjected to across PEEK and different grades of PEKK. This is shown in Figure 15, where each endothermic peak is labelled with the isotherm that the material has undergone. For example, the first peak labelled as 210°C occurs at approximately 220°C. The size of the endothermic peak is affected by the time the polymer is held at the isotherm for, increasing in size and slightly increasing in peak temperature with time as per Figure 16 [5]. The temperature at which the higher temperature endotherm (HTE) takes place, related to classic melting, is not affected by the annealing temperature or time.

The LTE in PEEK has been associated with different hypotheses: crystal reorganisation during heating, and the melting of less thermally stable crystallites [5,39,43,45,48]. Spherulites are formed of branching individual lamellae during primary crystallisation, with additional subsequent infilling between the lamellae. In PEKK, this has been attributed to the melting of this secondary structure within the spherulites [2,5,17,20,53]. It can therefore be established that PEKK crystallises with two different crystallisation processes: a primary crystallisation of amorphous material which takes place at the early stages of crystallisation, during which spherulitic entities are formed (as described in Section 2.3); and a secondary stage, during which interlamellar crystalline structures grow. These two processes are not independent: a structure developed by primary crystallisation must be established before secondary crystallisation can take place.

Quiroga Cortés et al. [5] also assess the crystallinity evolution of PEKK. A summary of this is presented in Table 4. As expected, crystallinity increases as the material is held for longer at the isotherm. With regards to the annealing temperature, results show that PEKK 60/40 reaches its highest crystallisation at around 250°C (even though further tests at 240°C would perhaps provide more clarity to this value). The total crystallinity achieved within the specified timeframe used in these experiments is heavily linked to the crystallisation kinetics of the material at different isothermal temperatures.

15

Table 4: Transition temperatures and crystallinity of PEKK 60/40 after annealing. Table excerpt from [5].

Holding temp.	Holding time	Low temp. endotherm	High temp. endotherm	Total crystallinity
210°C		221.0°C	300.0°C	22.2%
220°C		231.5°C	300.0°C	24.3%
230°C	60 min	241.5°C	299.5°C	26.2%
250°C		260.0°C	300.5°C	27.3%
260°C		270.0°C	301.5°C	26.5%
	5 min	251.5°C	300.0°C	22.5%
	10 min	252.5°C	300.0°C	23.4%
245°C	20 min	253.5°C	300.0°C	24.5%
	40 min	255.0°C	300.0°C	25.6%
	60 min	255.5°C	300.5°C	26.4%

Holding isotherms at different temperatures was further explored by Gardner et al. [17] with different grades of PEKK. The results of this can be observed in Figure 17. PEKK 90/10, 80/20 and 70/30 show a clear double-melting behaviour. However, PEKK 60/40 and 50/50 show a more complicated melting. This is likely due to the increase in meta- linkages, which, as discussed previously, increases chain flexibility. There are two relative rotations of phenyl rings across a meta- linkage, which may result in different, more complex packing interactions in PEKK grades with higher meta- linkage content [17]. On top of this, PEKK 50/50 is also a homopolymer, while the rest of the grades are random copolymers. This not only makes PEKK 50/50 the specimen with the highest flexibility, but also with the highest chain regularity, potentially complicating the crystallisation and melting behaviour of the material [17].

It is worth noting that the slightly more complicated melting behaviour observed in Gardner et al.'s results for PEKK 60/40 [17] is not visible in Quiroga Cortés et al.'s work [5]. This may be due to other differences in the polymers, such as polymer synthesis process, average molecular weight and molecular weight distribution, now that material suppliers are different for each article.
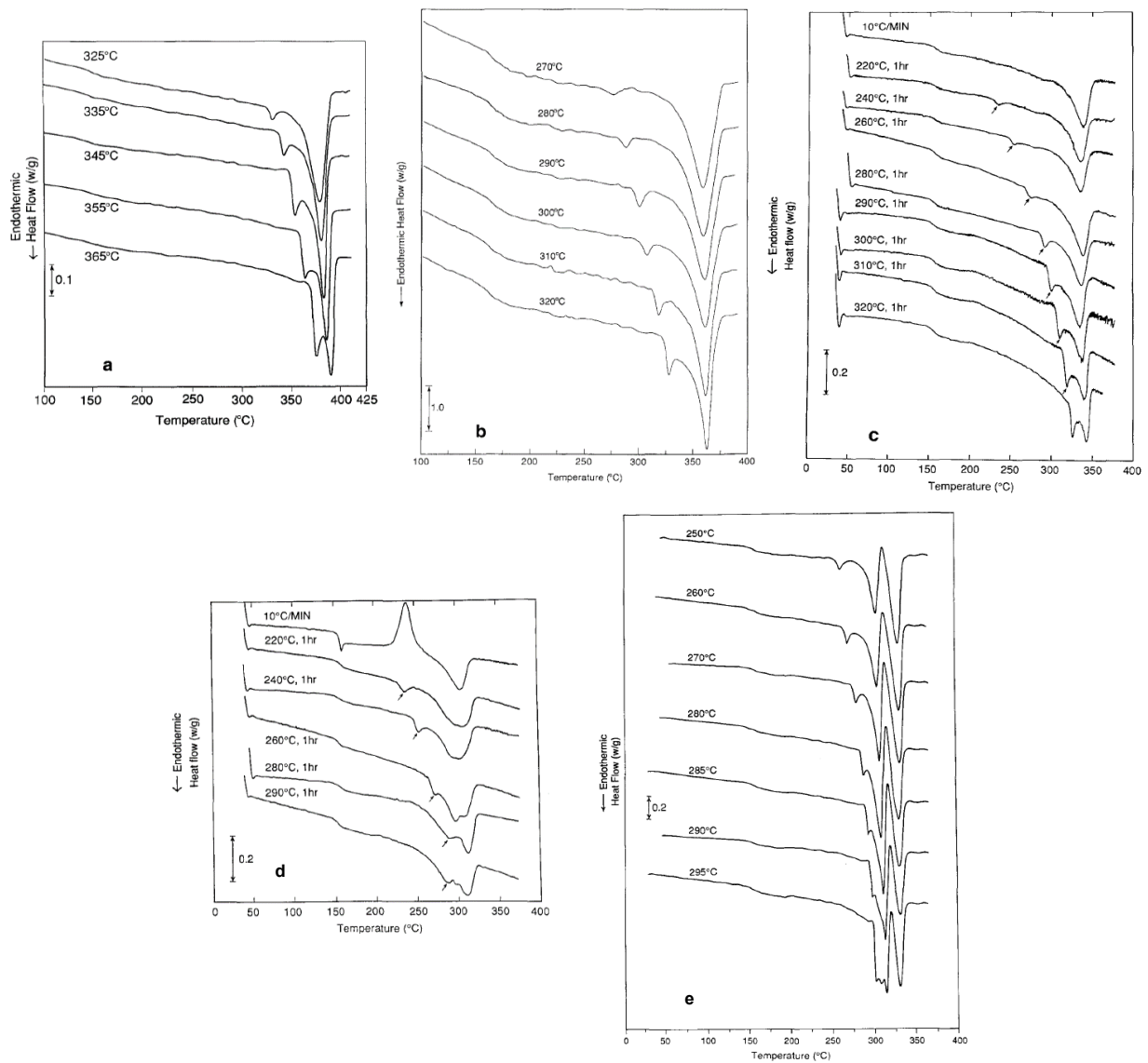
Figure 17: DSC scans of PEKK specimens annealed at different temperatures: (a) PEKK 90/10, (b) PEKK 80/20, (c) PEKK 70/30 (d) PEKK 60/40, (e) PEKK (50/50) [17].

In comparison to PEEK, overall crystallinity is lower in PEKK, which is to be expected due to PEEK's higher content of the more flexible and less bulky ether linkages, which facilitate faster crystallisation; as well as the exclusive para- linkages that PEEK has, enabling the polymer chain to be locally straight. In PEKK, particularly with lower T/I ratios, meta- linkages do not allow for this, hindering chain packing, as shown in Figure 3 [5,10,18,23,27].

3.2. Non-Isothermal Crystallisation

Crystallisation in any thermoplastic polymer is affected by the cooling rate that it undergoes. Assessing crystallisation under non-isothermal conditions is perhaps a more realistic way of understanding the crystallisation process in higher-paced manufacturing environments. Quiroga Cortés et al. [5] performed a thorough study on several grades of KEPSTAN PEKK supplied by Arkema, subjecting the materials to a variety of cooling rates after erasing any thermal history. The resultant DSC heating scans with

17

different cooling rates are shown in Figure 18, and crystallinities from each cooling rate are summarised in Table 5 below.
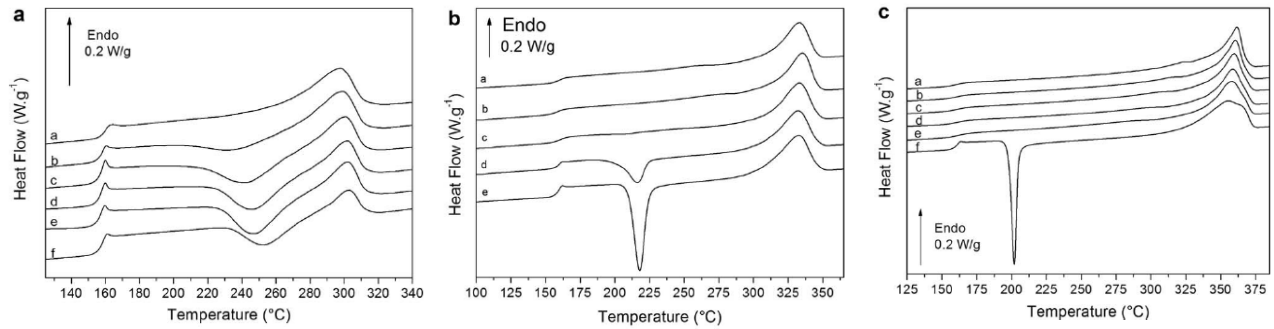
Figure 18: DSC thermograms of PEKK at 10°C/min after different cooling rates.
*Plot **a**, PEKK 60/40: (a) 2°C/min, (b) 5/C min, (c) 10°C/min, (d) 20°C/min, (e) 40°C/min, and (f) quenched.*
*Plot **b**, PEKK 70/30: (a)10°C/min, (b) 20°C/min, (c) 40°C/min, (d) 60°C/min, and (e) quenched.*
*Plot **c**, PEKK 80/20: (a) 5°C/min, (b) 10°C/min, (c) 20°C/min, (d) 40°C/min, (e) 60°C/min, and (f) quenched [5].*

Table 5: Crystallinity percentage for PEKK samples subjected to cooling at various cooling rates. Table excerpt from [5].

PEKK grade T/I ratio	Cooling rate	Crystallinity
KEPSTAN 6003 60/40	0.5°C/min	28.4%
	1°C/min	27.0%
	2°C/min	21.6%
	5°C/min	14.1%
	10°C/min	2.5%
	20°C/min	2.7%
	40°C/min	2.5%
	60°C/min	2.5%
	Quenched	0.5%
KEPSTAN 7003 70/30	10°C/min	27.7%
	20°C/min	28.1%
	40°C/min	25.2%
	60°C/min	15.8%
	Quenched	3.2%
KEPSTAN 8002 80/20	5°C/min	34.0%
	10°C/min	33.8%
	20°C/min	33.2%
	40°C/min	32.9%
	60°C/min	31.5%
	Quenched	7.1%

These results show, as expected, that a higher cooling rate results in a lower crystallinity percentage. A higher cooling rate inhibits any chain reorganisation that takes place when cooling from the melt, hindering crystal structure formation. This increases the amount of amorphous phase present, which undergoes cold crystallisation during subsequent heating. The cold crystallisation peak is therefore larger with a higher cooling rate [5]. PEKK with lower T/I ratios becomes progressively more susceptible to the cooling rate, and has a lower crystallisation, further reinforcing the discussion in Section 2.1.

Chang and Hsiao [38] briefly cover the effect of cooling rates on PEKK as well. The grade of the polymer is unknown, however, the melting temperature obtained (338°C) suggests that the T/I ratio may be approximately 70/30. Despite not reporting any quantitative values of crystallinity developed, their cooling DSC thermograms show a melt crystallisation exotherm occurring at progressively lower temperatures with higher cooling rates. This suggests that melt crystallisation requires a larger gap between melting and crystallisation temperatures (a larger supercooling) as the cooling rate increases [38]. The crystallisation start, peak and end temperatures are therefore strongly dependent on the cooling conditions, also observed in PEEK [40,54].

Similar to PEKK, the crystallisation percentage of PEEK decreases with an increase in cooling rate. However, the decrease is substantially smaller, particularly when compared to PEKKs with lower T/I ratios. As per the isothermal crystallisation analysis, PEEK also seems to obtain a higher crystallinity than PEKK when cooled at the same rate. This is due to the higher ether content and purely para-linkages that PEEK possesses, as discussed previously. Due to this high crystallinity, the cold crystallisation exotherm visible in many of the fast cooling rates of PEKK is not present in PEEK. Gao and Kim [21] in fact observe a small cold crystallisation exotherm for PEEK at 600°C/min cooling rate while achieving a crystallinity of 26%, and go up to 1500°C/min where a crystallinity of 17% was observed.

3.3. Crystallisation Kinetics in Composites and Effect on Mechanical Properties

The introduction of carbon fibres into PAEKs has been observed to have an effect on its crystallisation kinetics and transcrystalline interface. Literature covering the effect of this in PEKK, however, is minimal. This section will therefore include some reporting of PEKK in theses, but will mainly focus on published literature covering the effect of these inclusions in PEEK, particularly when discussing transcrystallinity.

Gao and Kim [21] obtained 1-5% lower overall crystallinities in CF/PEEK than in its neat counterpart when undergoing different cooling rates. They suggested this may be due to the presence of densely packed fibres suppressing spherulitic growth, as discussed previously. Velisaris and Seferis [34] explained this as being due to the presence of carbon fibres decreasing the extent to which the primary crystallisation process takes place, causing a drop in the final degree of crystallinity. They used different grades of PEEK in their work however (450P powder for neat PEEK, and APC2 tape for the composite, which is similar to 150P PEEK grade [19]), so a direct comparison may not be applicable. In the case of PEKK, Hsiao et al. [19] reported that the presence of fibres had little effect on the relative volume fraction crystallinity under isothermal conditions, possibly due to its rapid nucleation ability.

The impact of fibres on kinetics has been investigated to some extent. Hsiao et al. [19] reported once again that the inclusion of fibres had minimal impact on the crystallisation rate of PEKK under isothermal conditions, as shown by the very similar crystallisation peak times reported in Figure 19. On the other hand, higher fibre contents in Lee and Porter's work [29] with CF/PEEK showed faster kinetics than unreinforced PEEK under dynamic conditions, where the peak crystallisation temperature

shifted from 283°C at 0% carbon fibre volume content to 286°C at 18.5% carbon fibre volume content while cooling at 20°C/min.

A larger temperature range study is offered by Harris in their thesis [22], where they compared crystallisation kinetics of PEEK and CF/PEEK between 310°C and 318°C. They found that kinetics are similar at low isothermal temperatures, whereas PEEK composites crystallise faster at higher temperature isotherms. Harris attributed this behaviour to the fact that at higher temperatures, nucleation kinetics in the bulk will be low and the carbon fibres act as stress initiators for nucleation; whereas at lower temperatures, nucleation kinetics in the bulk are incentivised, and fibres hinder the matrix macromolecular chain mobility. This behaviour can be observed in Figure 20, where the half-times for the composite can be seen to be considerably lower at high temperatures, and closer to unreinforced PEEK at lower temperatures.
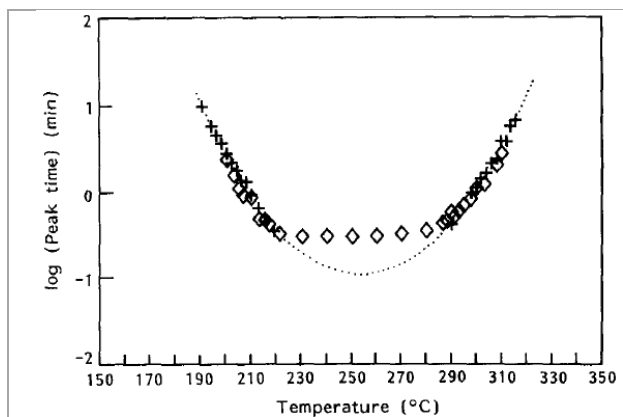
Figure 19: Crystallisation peak time vs. temperature for PEKK resin ◊ and its AS4/PEKK carbon fibre-reinforcement composite +. The dotted curve represents the fit from a second-order polynomial equation [19].
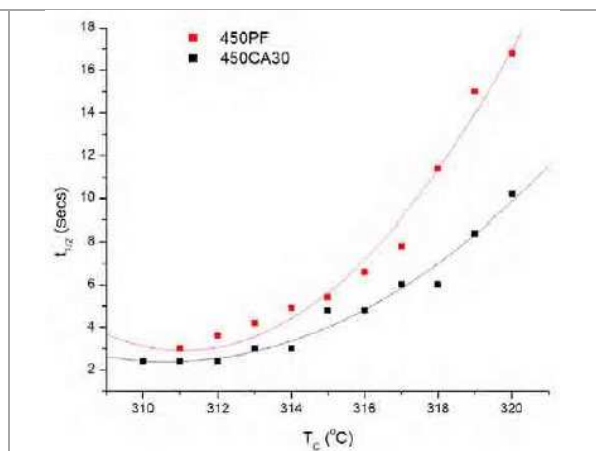
Figure 20: Comparison of half-time values for unreinforced PEEK (450PF in red) and CF/PEEK (450CA30 in black) [22].

A similar conclusion was reached by Choupin in their thesis work [31], where they observed kinetics of PEKK and CF/PEKK (grade 60/40) at a variety of isotherms, ranging from 200°C to 275°C. At temperatures above 265°C, crystallisation kinetics in the bulk are slower and thus the main crystallisation mechanism takes place on the carbon fibre surfaces, resulting in a faster crystallisation in the composite material; whereas at temperatures below 265°C, nucleation kinetics in the bulk dominate and the fibres play a lesser role, and therefore the difference in kinetics is smaller.

Primary crystallisation has overall been observed to be hindered by the fibre, resulting in less perfect crystalline entities and an increased secondary crystallisation.

The phenomenon of transcrystallinity, in particular, is also directly impacted by holding temperature and cooling rate. This is linked to the above discussion of Choupin's work [31], where high isothermal crystallisation temperatures coming from the melt favour the occurrence of transcrystallinity in PEKK, due to the carbon fibres acting as nucleation agents, whereas the opposite happens at low crystallisation temperatures. Similarly, slower cooling rates from the melt will allow for larger crystallisation growth from the fibre surface, and less nucleation from the bulk. Gao and Kim [21] observed a large amount of fibre nucleated spherulites in slow-cooled (1°C/min) AS4 CF/PEEK composites, where the developed crystallisation is well defined and larger in size, whereas fast-cooled (1000°C/min) specimens displayed

a mixture of smaller, isolated and fibre-nucleated spherulites. Tung and Dynes [55] also observed a noticeably developed transcrystalline region in slow-cooled samples (1.5°C/min), while that was not very apparent in fast-cooled samples (70°C/min, 2500°C/min) of CF/PEEK.

The presence of transcrystallinity is also dependent on the holding time of the material in the melt, now that this will determine the extent to which traces of previous spherulites or "defects" in the matrix are still present as nucleation sites. A longer holding time will increase the homogeneity in the bulk, leaving fewer nucleation sites available in the matrix and therefore allowing for a more developed transcrystalline region [29,56]. On the other hand, simply annealing a sample will create a high nucleation density and will not allow for any further development of transcrystallinity. This can be observed in Lee and Porter's work [29] shown in Figure 12 in Section 2.3, where the CF/PEEK sample held the longest in the melt (4 hours) developed a clear transcrystalline region, whereas the sample held for the shortest time (0.5 hours) developed a very high nucleation density in the matrix and no visible transcrystallinity.

The morphological impact that different processing conditions have on CF/PAEK composites also play a crucial role in the performance and failure mechanisms of the materials and their fibre-matrix interface. Gao and Kim [21] collected data on interfacial shear strength (IFSS) of identical AS4 CF/PEEK systems [57–60], which were found to vary widely (40-110 MPa) partly as a consequence of the different processing and testing conditions used. Overall, Gao and Kim [21] observed a much better fibre-matrix adhesion at slow cooling rates with fibre pull-out tests, these being characterised by brittle fracture with little matrix deformation along the fibre, and fast cooled specimens displaying extensive plastic yielding. This is observable in their SEM images in Figure 21, where ordered structures are visible on the fibre surface of the slow-cooled sample at 1°C/min, and a smooth surface in the fast cooled counterpart at 1800°C/min [21,56]. This is due to the time that the polymer is exposed to higher temperatures. PEEK molecules tend to uncoil further when undergoing slow cooling rates or higher temperature isotherms, and therefore get adsorbed more onto the fibre surfaces.
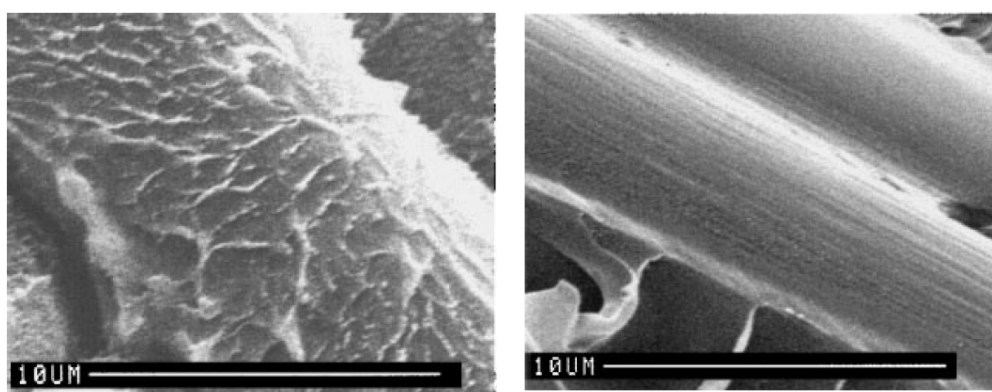
Figure 21: Scanning electron micrographs of fracture surfaces of CF/PEEK cooled at 1°C/min (left) and 1800°C/min (right) [21].

Gao and Kim's studies [21] compliment Saiello et al.'s findings [61] on how different isotherms affect fibre/matrix adhesion. They observed differences in the surfaces of cryo-fractured CF/PEEK samples that had undergone cold crystallisation at 180°C, or had been held in the melt and then crystallised at 320°C for 60 minutes each. SEM results showed some ordered structures in the matrix of the annealed

sample, as expected from holding in an isotherm, however the fibre surfaces were clean, indicating little fibre-matrix interaction (adhesive failure). On the other hand, the fibres of the specimen crystallised from the melt were still covered by the matrix after fracture, which could be observed to have some form of order (cohesive failure). These observations were in line with further SEM observations that they made with as-received amorphous (<5%) and crystalline (30%) CF/PEEK samples in the same work. Figures showing these results are available in their work [61].

The above discussion tackles the effect of fibre-matrix adhesion in general, but does not provide a focus on transcrystallinity in particular. In fact, despite the above findings, the effect of transcrystallinity on mechanical properties and interfacial strength is a topic of controversy. There is a consensus on its properties being different to that of the matrix bulk [21,30,62–64], however the results reported in literature are somewhat conflicting across different matrix materials. Chen and Hsiao [30] carried out micro-debonding tests on carbon fibres embedded in a PEKK matrix, prepared by heating a sandwich of matrix film and fibres. The test was performed by applying a stepwise compression loading on a single fibre until debonding takes place, identified by a microscope. They concluded that the presence of a transcrystalline region increases the strength of CF/PEKK by 40% when compared to its amorphous counterpart. Saiello et al. [61] agreed on the fact that having some form of crystalline fibre-matrix adhesion has a positive effect on the interface properties in comparison to having a fully amorphous interface.

When compared to bulk crystallinity, however, there is uncertainty regarding whether a transcrystalline region is beneficial for the composite's strength or not. Gao and Kim [21] proposed that the build-up of thermal stresses during the transcrystallisation process can reduce interfacial shear strength, whereas the presence of a transcrystalline region decreases the mismatch of moduli between fibre and matrix, improving the stress transfer across the interface and hence the composite's mechanical properties. This hypothesis is not supported uniformly across the available literature: Lustiger [36] compared the low and high modulus fibres discussed previously, showing that CF/PEEK systems with a transcrystalline region have a lower ILSS and transverse flexural strength, dropping by almost 25% and 50% respectively. This was further reinforced by visual inspection, where AS4 fibres (with no developed transcrystallinity) were well coated with the matrix material, while HMS fibres (which showed a transcrystalline region) appeared clean. On the other hand, Lee and Porter [29] concluded that a transcrystalline region in CF/PEEK systems results in twice the strength in transverse tensile tests when compared with other samples with no interface but of similar crystallinity.

Overall, the crystallisation kinetics of CF/PAEK systems and the effects of transcrystallinity need further research. While some literature is available reporting differences in crystallisation kinetics between the two, this is either not peer-reviewed (such as the theses by Choupin and Harris) or is not in-depth. Further to this, literature focusing on PEKK in particular is minimal. Even though PEEK and PEKK behave comparably, further research is needed in CF/PEKK systems in order to further quantify and understand this material's behaviour.

3.4. Matrix-dominated mechanical properties

This section offers a brief review of the mechanical properties of unreinforced PEKK, PEEK and matrix-dominated properties of CCF/PEKK and CF/PEEK when undergoing a range of different manufacturing cycles observed by several authors. As the impact of crystallinity on the composite's performance has already been discussed in Section 3.3, this section will focus on providing a collection of data available in literature, and discussion is kept to a minimum.

While there is limited data available on the impact of crystallinity on the performance of CF/PEEK or CF/PEKK, some literature does cover this in the case of unreinforced PEKK and PEEK. This is the case of Figure 22 and Figure 23, adapted from Choupin et al. [65] and Gao and Kim [21] respectively, which show tensile properties of PEKK and PEEK. While the samples in each figure have been prepared differently (the PEKK samples underwent different isothermal holds, whereas the PEEK samples underwent various cooling rates), the plots still allow for a comparison between mechanical performance and crystallinity. A higher crystallinity induces a higher stiffness in both materials, due to the presence of ordered crystallites and thicker lamellae, which hinder any slipping of material in the crystal blocks [21]. A lower crystallinity therefore results in a more ductile material, with lower strength and stiffness.
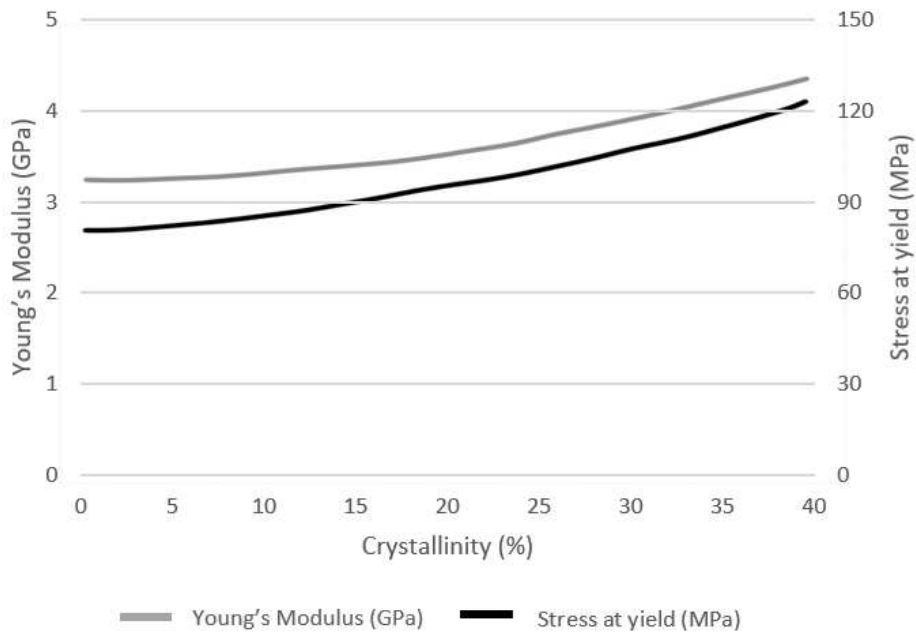

Figure 22: Young's modulus and stress at yield vs. crystallinity at room temperature of neat PEKK crystallised at 230°C from the glassy state. Adapted from [65].
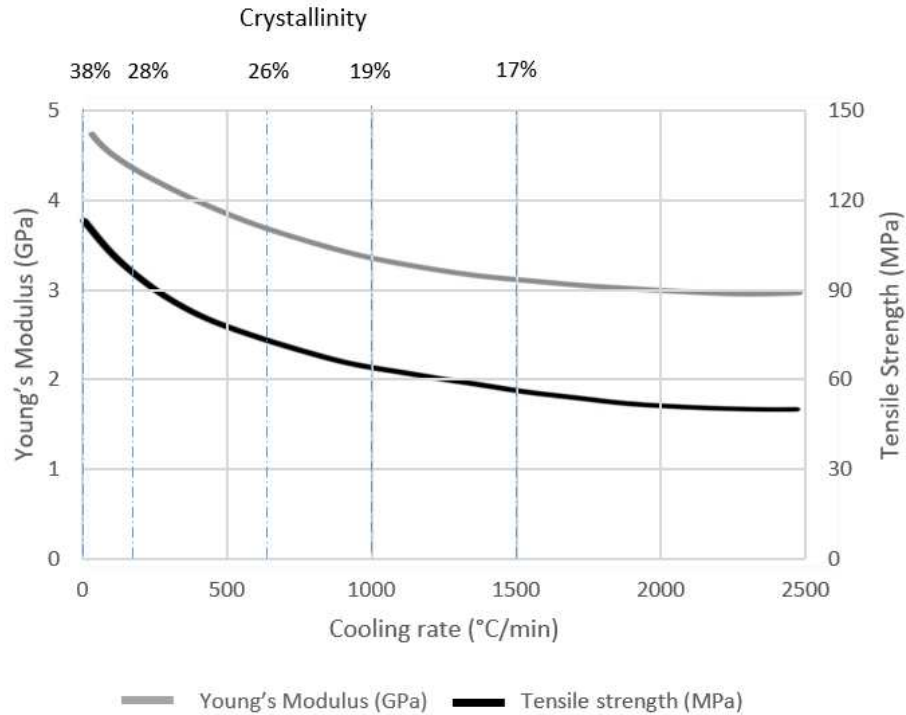
Figure 23: Tensile strength, Young's modulus and crystallinity of neat PEEK as a function of cooling rate. Adapted from [21].

A study covering matrix-dominated properties of CF/PEKK composites was performed by Choupin in their thesis work [31], the results of which are shown in Table 6. While these do not show a spectrum of crystallinities and the impact of this on matrix behaviour, they show the difference between fully crystallised and amorphous matrix composites where possible. In PEKK 6002 (T/I ratio 60/40), a clear decrease in the properties can be observed for the amorphous samples, which becomes much more distinct when tested at 180°C. More information on this can be found in their work [31].

Table 6: Crystallinity, shear modulus and Young's modulus of ±45° of PEKK composites manufactured under different conditions, tested at room temperature and 180°C. Adapted from [31].

Material	Processing conditions	Crystallinity	Shear modulus (±45° tensile test)		Young's Modulus (±45° tensile test)	
			Test temperature		Test temperatures	
			T_{room}	180°C	T_{room}	180°C
CF/PEKK 6002	Autoclave (10 min at 360°C, followed by 2h at 230°C)	30%, fully crystallised	5.6	0.53	16.5	1.9
	Press (10 min at 360°C, followed by 2h at 230°C)	30%, fully crystallised	5.1	0.49	17.3	1.7
	Press (10 min at 360°C, followed by 20°C/min cooling rate)	5%, amorphous	3.7	0.046	15.4	0.33
CF/PEKK 7002	Autoclave (10 min at 380°C, followed by 20°C/min cooling rate)	33%, fully crystallised	4.4	0.39	17.9	1.6
	Press (10 min at 380°C, followed by 20°C/min cooling rate)	28%, fully crystallised	4.6	0.33	17.8	1.2

Choupin [31] also performed high (from the melt) and low (from the glassy state) isothermal holds to

observe potentially high and low amount of transcrystalline phases respectively. Due to low residual nuclei, the isothermal hold from the melt would allow for a transcrystalline region to form, whereas when crystallising from the glassy state, this is unlikely to be the case. The results of ±45° tensile tests are available in Table 7. The shear modulus and Young's modulus can be observed to be 22% and 2% higher at room temperature, and 12% and 38% higher at 180°C respectively for CF/PEKK composites crystallised at a higher temperature. This behaviour could be attributed to a higher amount of transcrystalline region present in the sample crystallised at a higher temperature, resulting in a better load transfer between fibre and matrix, as per the discussion in Section 3.3.

Table 7: Crystallinity, shear modulus and Young's modulus of ±45° of PEKK composites held at different isothermal conditions, tested at room temperature and 180°C. Adapted from [31].

Material	Processing conditions	Crystallinity	Shear modulus (±45° tensile test)		Young's Modulus (±45° tensile test)	
			Test temperature		Test temperature	
			T_{room}	180°C	T_{room}	180°C
CF/PEKK 6002	Autoclave (10 min at 360°C, followed by 4h at 260°C)	28%, fully crystallised	4.7	0.51	17.76	2.4
	Press (10 min at 360°C, followed by 20°C/min to room temperature, then 4h at 200°C)	30%, fully crystallised	3.68	0.45	17.44	1.5

Outside of the above, no studies covering matrix-dominated properties of CF/PEKK composites were found, and so a compilation of various articles on CF/PEEK is offered in Table 8 instead.

Table 8: Compilation of matrix-dominated properties of CF/PEEK offered by various authors.

Material	Crystallinity/processing conditions	Crystallinity	Transverse tensile strength (MPa)	Transverse flexural strength (MPa)	Interlaminar shear strength (MPa)	Interfacial shear bond strength (MPa)	Ref.
AS4/PEEK	Hot pressed in a vacuum furnace at 450°C at 2MPa, for 10-40min (see to the right). Followed by 400°C/min cooling. 10 min					49.9	[21, 58]
	20 min					55.4	
	30 min					73.2	
	40 min					96.7	
AS4/PEEK	Molten at 390. Followed by: Quenched in iced water					74	[21, 66]
	Slowly cooled in air					97	
	Annealed at 320°C for 60 min, then quenched in iced water					112	
AS4/PEEK	Unknown			152	38.9		[36]
HMS/PEEK	Unknown			76.4	29.7		
T300 CF/PEEK	30 min preheating at ambient pressure 390°C, followed by compression moulding at 390°C at 2 MPa for 30 min, and cooled at different rates: 0.6°C/min	45%	60				[29]
	7°C/min	42%	63				

	100 min preheating at ambient pressure 390°C, followed by compression moulding at 390°C at 2 MPa for 30 min, and cooled at different rates:	0.6°C/min	36%	106				
		7°C/min	43%	111				
AS4/PEEK	Hot pressed at 400°C at 1MPa for 60 min, followed by cooling at different rates (pressure removed for cooling):	3°C/min (9% void content)			60*			[67]
		10°C/min (6% void content)			90*			
		175°C/min (4% void content)			110*			
AS4/PEEK	Hot pressed at 400°C for 60 min at 1MPa, followed by 3°C/min cooling rate at different pressures:	Ambient pressure		55				[68]
		0.2MPa		125				
		0.4MPa		130				
		1MPa		120				
APC2 (CF/PEEK tape)	Held at 400°C for 15 min, then cooled at different rates:	0.33°C/min	31%		172	117		[69]
		22-23°C/min	26%		154	108		
AS4/PEEK	Held 420°C for 15 min, then cooled at different rates:	0.33°C/min	36%		114	103		
		22-23°C/min	26%		146	101		
IM7/PEEK	Autoclave – held at 375°C for 20 min at 7 bar, then cooled at 3°C/min		40%			112		[70]
	Automated tape placement – lay down speed 8m/min, roller pressure 1.2 bar. (High heating and cooling rates)		18%			78		
AS4/PEEK	Held at 400°C for 10 min in an oven, then cooled between 1-1500°C/min.		14-38% (see Figure 24)			50-80 (see Figure 24)	75-115 (see Figure 24)	[21]

* = while these results may seem that a slower cooling rates results in a lower performance, this is actually a consequence of the void content of the different laminates, which is highest at the 3°C/min (12%) sample and lowest at the 170°C/min (4%).

As seen in Table 8, a thorough evaluation of matrix mechanical properties as a function of crystallinity under different processing conditions is scarce. Some papers do mention a correlation between superior mechanical properties with a higher crystallinity content [58,69], but only a few of them cited in Table 8 offer crystallinity values for the different processing cycles that their samples underwent. None of these studies offer a diligent review of the impact of thermal cycles (varying holding times, varying cooling rates) on composite crystallinity and their consequent effect on the matrix performance. An exception to this is Gao and Kim's paper [21] mentioned in the previous paragraph ad in the last row of Table 8, which does offer information on the variation of ILSS, IFSS and crystallinity with respect to cooling rate, shown in Figure 24.
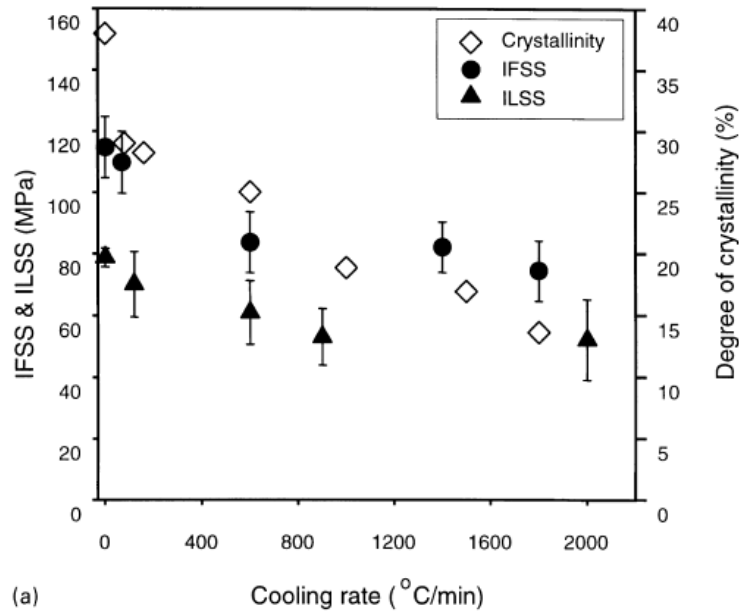
Figure 24: Comparison of IFSS, ILSS and degree of crystallinity as a function of cooling rate [21].

Thorough studies on the impact of thermal cycles on the crystallinity and performance of composite matrices are essential for the better understanding of how thermoplastic composite materials can be reliably used in industry. This is perhaps less significant with PEEK as it is a fast-crystallising material, but with PEKK, particularly grades with lower T/I ratios (and therefore slower crystallisation kinetics), the thermal cycle that the material undergoes is paramount to its crystallinity and mechanical behaviour.

4. Modelling of Crystallisation Kinetics

As has been discussed in Section 3, the dual crystallisation mechanism that takes place in PEKK is paramount in the understanding of kinetics. When plotted against time, the evolution of crystallinity can be observed to take a sigmoidal shaped curve. In the initial stages of crystallisation, spherulites start to nucleate and grow, followed by a faster spherulitic growth period, namely primary crystallisation. Once spherulites begin to impinge on each other, crystallisation slows down, but even after maximum volume of crystallisation has been achieved, crystallisation continues in the form of interlamellar crystalline structures. This is known as secondary crystallisation, corresponding to the upper tail of the curve.

Modelling this double crystallisation behaviour in PEKK (and other PAEKs) has been the object of several studies, and an overview of several models is presented in this section. The main background theory of polymer crystallisation kinetics is outlined first, followed by an explanation of the most relevant models and a discussion of any similarities and discrepancies found in literature, as well as any extra commentary on reinforcement with carbon fibres where literature is available. Isothermal crystallisation kinetics will be discussed first, followed by non-isothermal crystallisation kinetics. Notation is consistent throughout the entirety of Section 4, and so may not be the same as that used in the discussed papers. Finally, a brief overview of two transcrystallisation simulations is given.

4.1. Isothermal Crystallisation Kinetics

The initial stages of crystallisation, where crystals grow independently, has often been modelled in terms of the Avrami equation [71]:

	$$\alpha(t) = 1 - \exp(-kt^n)$$	(4.1)

where the quantity $\alpha(t)$ is a measure of the relative volume fraction of crystallinity at time t, k is the crystallisation rate constant, and the Avrami exponent n is related to the nature of crystal growth for the first mechanism. Assessment of whether the Avrami equation correctly models the crystallisation process can be done by plotting $\log[-ln(1-\alpha)]$ against $\log t$. If successful, the plot would result in a straight line of gradient n and intercept $\log k$.

The Avrami exponent n is understood to be equal to the number of directions that crystal growth takes place with instantaneous nucleation, leading to rods, discs or spheres for $n = 1$, 2 or 3 respectively. However, a value of 2 for the Avrami exponent could also be associated with a one-dimensional growth with sporadic nucleation; which is how up to an exponent of 4 can be achieved with 3-dimensional growth and sporadic nucleation. The relation between the exponent, geometry and nucleation type is shown in Table 9. However, it is worth noting that the Avrami equation should be used with caution, now that non-integer values for n_1 are often found to fit experimental data, and the shape of the morphological unit predicted is not always correct [2,28]. This will be observed in the results obtained for PEEK and PEKK by several authors in this section. Potential reasons for this can be that nucleation occurs as a combination of the instantaneous and sporadic mechanisms, as well as crystallisation growth not being exclusively spherulitic for instance, but rather being a mix of structures of different dimensions [34,72,73]. The latter may be particularly relevant in the case of composites where a one-dimensional growth may occur at the fibre-matrix interface, as described in Section 2.4.

Table 9: Relation between the Avrami exponent and the morphological unit. Adapted from [2,74].

Growth unit	Geometry	n_1 with instantaneous nucleation	n_1 with sporadic nucleation
Spherulites	3D	3	4
Discs	2D	2	3
Rods	1D	1	2

The crystallisation rate constant k varies with the growth unit and nucleation type, and can be expressed as a function of the initial number of potential nuclei N and the crystal growth rate G. Table 10 below provides a summary of these.

Table 10: Relation between crystallisation rate constant k and the morphological unit. Adapted from [2,20].

Growth unit	Instantaneous nucleation	Sporadic nucleation
Spherulites	$\dfrac{4\pi NG^3}{3}$	$\dfrac{\pi NG^3}{3}$

Discs	$\pi N G^2$	$\dfrac{4\pi N G^2}{3}$
Rods	NG	$\dfrac{1}{2}NG$

In the case of PEKK, as mentioned in Section 2.3, nucleation is instantaneous.

According to Hoffman and Lauritzen theory [75], the crystal growth rate in polymers can be expressed as follows:

$$G_i(T) = G_{0i}\exp\left(-\frac{U^*}{R(T - T_\infty)}\right)\exp\left(-\frac{K_{gi}}{T \times \Delta T \times f}\right) \qquad (4.2)$$

G_{0i} is a pre-exponential factor independent of temperature. The first exponential term corresponds to the contribution of macromolecular chain diffusion in the melt, where U^* is the activation energy of the molecular transfer from the melt to the crystal interface, T_∞ is the temperature below which diffusion stops ($T_\infty = T_g$ - 30 K), and R is the gas constant. The second exponential term contains the contribution of the nucleation process, where K_{gi} is the activation energy of nucleation for a crystal with a critical size, ΔT is the degree of supercooling ($\Delta T = T_m{}^0 - T$) with $T_m{}^0$ as the equilibrium melting temperature, and f is a correction coefficient accounting for the temperature dependence of the melting enthalpy ($f = 2T/(T_m{}^0 + T)$). The index i for G_i, G_{0i}, and K_{gi} is equal to 1 for primary crystallisation and 2 for secondary crystallisation. Further details of the Hoffman Lauritzen theory can be found in their work [75], and specifically applied to PEKK in [2,20,72].

It is also worth noting that the use of the Avrami equation alone completely ignores the existence of a secondary growth stage, which has been repeatedly observed in PEKK and PEEK. This is observable in Velisaris and Seferis' work on PEEK [34], where the Avrami plot shown in Figure 25 displays two competing crystallisation mechanisms, and therefore two distinct gradients corresponding to different Avrami exponents. Choupin et al. [2] show similar behaviour for PEKK, as per Figure 26.
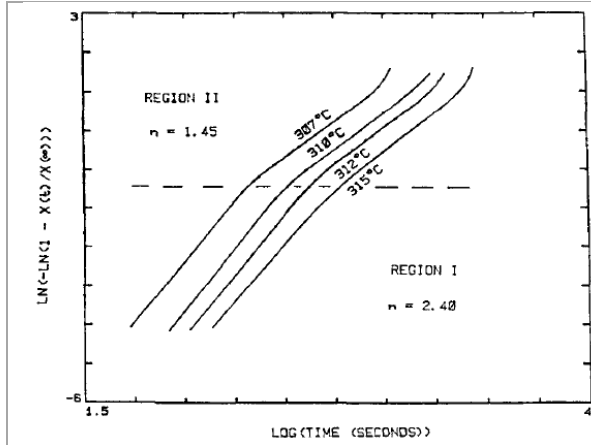
Figure 25: Avrami crystallisation plots for the isothermal crystallisation of neat PEEK at 307°C, 310°C, 312°C, 315°C, showing the existence of two competing crystallisation processes [34].
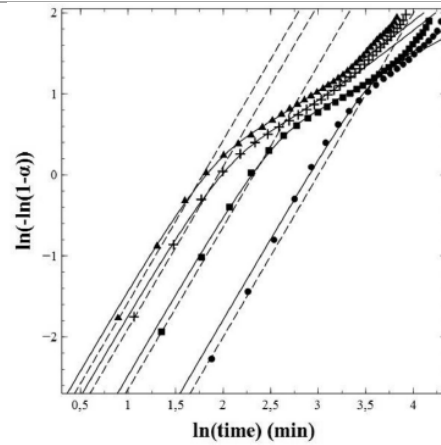
Figure 26: Double logarithm vs. ln(time) (from left to right: 230°C, 220°C, 210°C, 200°C), Avrami model (dashed curves) and Hillier model (solid curves, discussed below) for PEKK 60/40 isothermal crystallisation from the melt [2].

Velisaris and Seferis [34] tackled this by proposing two separate Avrami crystallisation processes taking place in parallel, as per Equation (4.3), which they tested on both unreinforced and CF reinforced PEEK.

$$\alpha(t) = w_1 \alpha_1(t) + w_2 \alpha_2(t) \qquad (4.3)$$

which, substituting for α_1 and α_2:

$$\alpha(t) = w_1[1 - \exp(-k_1 t^{n_1})] + w_2[1 - \exp(-k_2 t^{n_2})] \qquad (4.4)$$

In the above equations, w_1 and w_2 are the weight factors corresponding to primary and secondary crystallisation respectively, providing the relative importance of each crystallisation mode ($w_1 + w_2 = 1$). All quantities with subscripts 1 and 2 refer to primary and secondary crystallisations respectively. Using 2.5 and 1.5 for n_1 and n_2 respectively (which provided the best fit to their data), they concluded that the model provided a good description of the crystallisation process for both neat and fibre-reinforced PEEK, achieving an average deviation from experimental data of 4%. It was observed that both rate constants for CF/PEEK were higher than that for its neat counterpart. As previously mentioned in Section 3.3, however, the PEEK grades used by Velisaris and Seferis in the neat and composite PEEK systems were different [19]. Crystallisation kinetics are therefore not comparable between the two.

Prior to this, Hillier [53] postulated a different model, where a primary Avrami type crystallisation took place followed by a first-order crystallisation process ($n_2 = 1$) growing from the primary crystallisation. Equation (4.5) shows the proposed expression for secondary crystallisation, and Equation (4.6) provides the overall crystallisation.

$$\alpha_2(t) = \int_0^t \alpha_1(\tau) \times \frac{\mathrm{d}}{\mathrm{dt}}[1 - \exp(-k_2(t - \tau)^{n_2})]d\tau \qquad (4.5)$$

$$\alpha(t) = w_1[1 - \exp(-k_1 t^{n_1})] + w_2 k_2 \int_0^t [1 - \exp(-k_1 \tau^{n_1})] \times \exp[-k_2(t - \tau)] d\tau \qquad (4.6)$$

30

Here, τ is the time at which a volume element has been included in the lamellae and secondary crystallisation begins. This model differs from the one Velisaris and Seferis [34] proposed, since the Hillier model assumes that this secondary crystallisation occurs after time τ, as opposed to both growths taking place independently and simultaneously from $t = 0$.

These two models were tested on PEKK and CF/PEKK by Hsiao et al. [19], who concluded that, after a modification of the exponent of the secondary crystallisation, the Hillier model provided a better fit than the Velisaris Seferis model. This was because the Hillier model has a better physical reasoning to describe the secondary crystallisation taking place within lamellae, as some primary crystallisation must exist before the secondary step begins. In this modified Hillier model, the secondary crystallisation is not assumed to be of the first order, and therefore the total crystallinity is:

$$\begin{aligned} \alpha(t) = w_1[1 - \exp(-k_1 t^{n_1})] \\ + w_2 k_2 n_2 \int_0^t [1 - \exp(-k_1 \tau^{n_1})] \times (t - \tau)^{n_2 - 1} \exp[-k_2(t - \tau)] \, d\tau \end{aligned} \qquad (4.7)$$

In order to identify the relative crystallinity and crystallisation kinetics parameters, the model must be fitted to the relative crystallinity, which can be calculated via the integration of heat flows measured using DSC:

$$\alpha(t) = \frac{\int_0^t Q(t) \, dt}{\int_0^{t_\infty} Q(t) \, dt} \qquad (4.8)$$

where $Q(t)$ is the heat flow measured at time t, and t_∞ is the time when the polymer is fully crystallised. This integration becomes a challenge to perform due to unstable heat flow signals resulting from the DSC switching from heating/cooling to isothermal. This is reflected as a shortening of the beginning of the crystallisation peak. This truncation becomes more prominent with lower temperature isotherms from the melt, and at temperatures at which higher crystallisation kinetics are favoured. An example of this is shown in Figure 27, where kinetics are faster at 230°C, resulting in a shorter peak as indicated by the arrows. This was commented on in Hsiao et al.'s work [19], and was later identified by Choupin et al. [2].

To tackle this, Hsiao et al. [19] simply used the results where the instrumental fluctuations did not interfere with the crystallisation signal. They found the Avrami exponents to be 4 and 2 respectively, representing a nucleation growth that is assumed to be three-dimensional and sporadic (time-dependent) during primary crystallisation, and two-dimensional or diffusion-controlled in the secondary stage. This is in disagreement with what Hillier previously assumed, where secondary crystallisation obeys a first-order law ($n_2 = 1$). Hsiao et al. argued that this assumption may oversimplify the secondary stage. Figure 28 demonstrates when primary and secondary crystallisation develop as per this modified Hillier model. In this study, the inclusion of carbon fibres in PEKK was not found to have an effect on the crystallisation rate constant or the relative volume fraction crystallinity for each crystallisation stage.
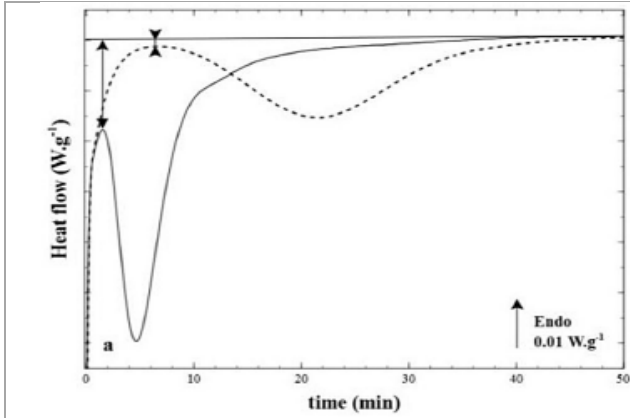
Figure 27: PEKK 60/40 DSC thermograms during isothermal crystallisation from the melt at 230°C (solid line) and 210°C (dashed line) [2].
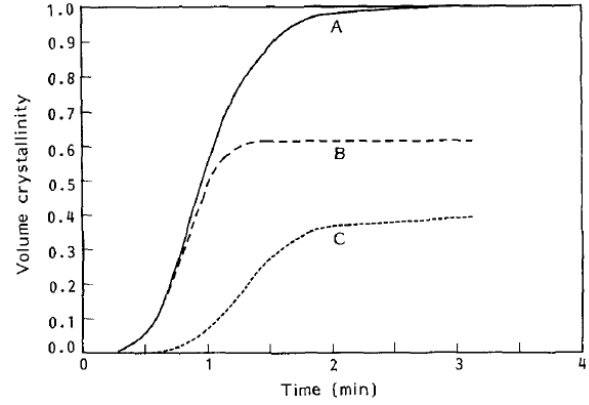
Figure 28: Isotherm of total volume crystallinity of PEKK (A) separated into a primary volume crystallinity (B) and a secondary volume crystallinity (C). The data were obtained from an isotherm at 298°C [19].

This initial truncation of the crystallisation signal proved to be a larger problem in Choupin's work on neat PEKK as shown in Figure 27, which was initially tackled by the introduction of an induction time [2]. This was defined by the intersection of the baseline and the extrapolation line of the crystallisation peak beginning, without which the model coefficients were not able to provide a good fit of the experimental data. This method produced an Avrami exponent of approximately $n_1=2$, however, which contradicted their microscopic observations of spherulitic entities as this exponent suggests lower dimensional growths (instantaneous nucleation with disc-like growths or sporadic nucleation with rod-like structures).

Furthermore, Choupin et al. suggested in later work [20] that the introduction of a crystallisation induction time is inconsistent with overall crystallisation kinetics theories, and proposed a further modification to the Hillier model. This new method considers only reliable DSC measurements and does not need extrapolation, called the derivative Hillier method. A more thorough explanation of the following derivation is available in their paper [20].

Equation (4.8) can be differentiated to obtain

$$\frac{d\alpha(t)}{dt} = \frac{Q(t)}{\int_0^{t_\infty} Q(t)dt} = \frac{Q(t)}{\Delta H_m} \tag{4.9}$$

where ΔH_m is the total melting enthalpy.

The derivatives of the primary crystallisation and secondary crystallisation rate equations (Equation (4.1) and (4.5)) are as follows:

$$\frac{d\alpha_1(t)}{dt} = k_1 n_1 t^{n_1-1} \exp(-k_1 t^{n_1}) \tag{4.10}$$

$$\frac{d\alpha_2(t)}{dt} = k_2 n_2[1 - \exp(-k_1 t^{n_1})] + $$
$$k_2 n_2 \int_0^t [1 - \exp(-k_1 \tau^{n_1})] \times \exp[-k_2(t-\tau)^{n_2}] \times [(n_2-1)(t-\tau)^{n_2-2} - k_2 n_2 (t-\tau)^{n_2-2} d\tau \tag{4.11}$$

The derivative of the total crystallinity is therefore

$$\frac{d\alpha(t)}{dt} = w_1 \frac{d\alpha_1(t)}{dt} + w_2 \frac{d\alpha_2(t)}{dt} \qquad (4.12)$$

with w_1 and w_2 corresponding to the weight factors for the primary and secondary crystallisation respectively. Choupin et al. [20] found the best fits to take place when $n_2 = 1$, simplifying Equations (4.10) - (4.12) to:

$$\frac{d\alpha(t)}{dt} = w_1 k_1 n_1 t^{n_1-1}(1 - \alpha_1(t)) + w_2 k_2(\alpha_1(t) - \alpha_2(t)) \qquad (4.13)$$

Choupin et al. [20] tested this model on neat PEKK 60/40 and 70/30 (KEPSTAN 6002 and 7002 respectively, by Arkema), in order to validate it under different crystallisation rates. The same Avrami exponents for primary crystallisation was chosen for both samples, $n_1 = 3$ and $n_2 = 1$, which is in line with the instantaneous, nucleation growth of spherulitic nature observed in PEKK. They also performed parameter modelling according to Hoffmann and Lauritzen theory as discussed previously, and appropriate crystallisation rate constants k_1 and k_2 were selected as per Table 10. Further details of this can be found in Choupin et al.'s work [20]. Their findings can be summarised in the time-temperature-transformation diagrams for PEKK shown below.
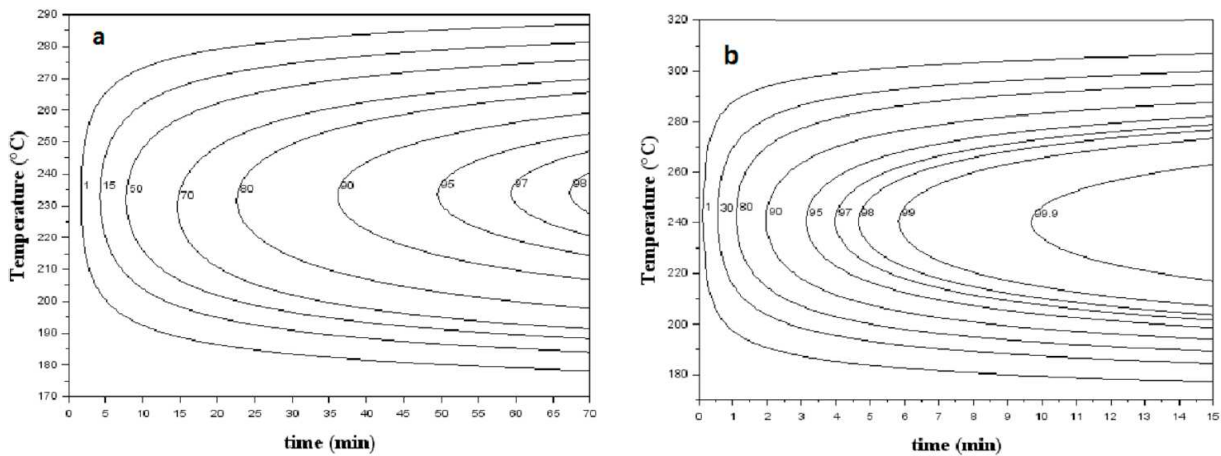

Figure 29: Time-temperature-transformation diagram of the relative crystallinity of PEKK (a) 6002 and (b) 7002 crystallised from the melt [20].

The same model (derivative Hillier) was later implemented by Chelaghma et al. [72] on neat PEKK 70/30 (KEPSTAN 7003 by Arkema), where n_1 was also found to be 3, but a different secondary exponent was obtained, $n_2 = 2.7$. Neither Choupin et al. nor Chelaghma et al. modelled kinetics of CF/PEKK composites.

The discrepancy on n_1 between Hsiao et al. [19], Choupin et al. [20] and Chelaghma et al. [72] lies in the nature of the nucleation of PEKK: Hsiao et al. [19] defend that the nucleating density is clearly a function of time as observed in thermal optical analysis (hence sporadic), and therefore as per Table 9, should follow that $n_1 = 4$. On the other hand, Choupin et al.'s optical microscopy results in Figure 11 [2]

33

depict crystalline entities of the same size, and therefore instantaneous nucleation can be assumed, which is, for spherulitic growth, $n_1 = 3$ [20]. Chelaghma et al.'s hot stage microscopy studies [72] also demonstrate instantaneous nucleation. The difference between the models used by Hsiao et al. [19] (Modified Hillier model) and Choupin et al. [20] and Chelaghma et al. [72] (derivative Hillier model) may be the reason as to why one constant fits better, and therefore has been selected over the other.

The discrepancies regarding n_2 are perhaps less conclusive. Hsiao et al.'s selection for $n_2 = 2$ [19] is somewhat arbitrary, but argue that Hillier's initial choice of $n_2 = 1$ [53], indicating that secondary crystallisation within the spherulite follows first-order growth, may be an oversimplification. The value $n_2 = 1$ was used by Choupin et al. as well [20], who simply selected the exponent which showed the best fit with the derivative Hillier model, and therefore represents 1-dimensional growth. Chelaghma et al. [72] however identified n_2 as 2.7, and suggests that the secondary crystallisation mechanism is not necessarily related to a unique process, but the formation of structures of different dimensions.

With regards to the proportion in which each of these crystallisation stages is observed in PEKK, the literature discussed above agrees on the secondary crystallisation becoming more prominent with higher isothermal crystallisation temperatures. The w_1/w_2 ratio varies with PEKK's T/I ratio and molecular weight. Choupin et al. [20] found a consistent decrease in primary crystallisation of PEKK 60/40 with an increase in temperature, whereas with PEKK 70/30 its value seemed considerably more constant. This could be attributed to a more organised chain packing as a consequence of the higher para- linkage presence, as discussed in Section 2.1. When using PEKK 70/30 of a lower molecular weight, Chelaghma et al. [72] found w_1 to decrease more significantly. Hsiao et al. [19] also observed a consistent decrease of w_1 with temperature in their PEKK samples (believed to be 70/30, by DuPont). There are discrepancies in the range of these values, likely due to slight differences in the chosen models and parameters as discussed above, as well as in the grade of PEKK. But overall, w_1 has been observed to vary between 0.9 and 0.55 for PEKK 70/30 in an isothermal temperature range of 270-310°C; and between 0.7 and 0.4 in an isothermal temperature range of 200-275°C for PEKK 60/40.

With the help of the models, Choupin et al. [20] plotted the variation of k_1 and k_2 for both PEKK 60/40 and PEKK 70/30 (Arkema), finding the fastest kinetics to take place at 235°C and 245°C respectively. Both crystallisation stages achieved this peak at the same temperatures for each grade. Hsiao et al. [19] found this temperature to be 255°C for PEKK 70/30 (DuPont), again, likely due to variation in molecular weight.

Implementation of isothermal crystallisation kinetics models on carbon fibre/PEEK and PEKK composites is sparse – from the above literature, Velisaris and Seferis [34], as well as Hsiao et al., [19] obtained successful fits on composite systems with the models they previously implemented on unreinforced PEEK and PEKK. Choupin also did this in their thesis work [31], and found that using the same primary Avrami exponent as he used for unreinforced PEKK ($n_1 = 3$) provided a good fit for high isothermal temperatures, whereas for lower temperatures, using $n_1 = 2$ created a more successful fit. The reason for this has been discussed in detail in Section 3.3, but at higher temperatures, crystallisation kinetics in the bulk are considerably slower. This results in the main crystallisation mechanism occurring on the carbon fibre surfaces, where the high nucleation density can cause impingement and therefore an epitaxial growth rather than spherulitic, reducing the value of the Avrami exponent.

34

Regardless, further investigation is necessary to verify the suitability of the discussed models, particularly the ones developed in the more recent years, now that there is little literature covering the implementation of these in unreinforced PEKK, and virtually none on CF/PEKK.

Overall, the understanding of the primary crystallisation of PEKK seems to be better established, and a consensus on spherulitic growth has been reached. There seem to be some discrepancies in the literature on whether the nucleation process is instantaneous or sporadic, but recent literature leans in favour of the former. Understanding of the secondary crystallisation mechanism is less clear however, due to it not being observable by microscopy methods. The model adaptations to accommodate for this are somewhat novel, particularly the derivative Hillier model. Investigation of the crystallisation kinetics of CF/PEKK is sparse for older models (Velisaris-Seferis, modified Hillier), and non-existent for the newer models (derivative Hillier). Further work needs to be carried out in this ambit in order to better understand the secondary crystallisation kinetics of PEKK, and the overall crystallisation kinetics process for CF/PEKK.

4.2. Non-Isothermal Crystallisation Kinetics

Available literature of models for non-isothermal crystallisation kinetics is considerably sparser than the isothermal counterpart. Several models have been developed based on the Avrami equation, such as the Nakamura [76] and Ziabicki [77] models, where non-isothermal crystallisation is predicted using isothermal crystallisation data; a differential Nakamura model, proposed by Patel and Spruiell [78]; or the Ozawa model, where an infinite number of isothermal steps are assumed to form the non-isothermal process [79]. The Ozawa model is perhaps the most attempted one on non-isothermal crystallisation kinetics model on our materials of interest (as explained below), and takes the following form:
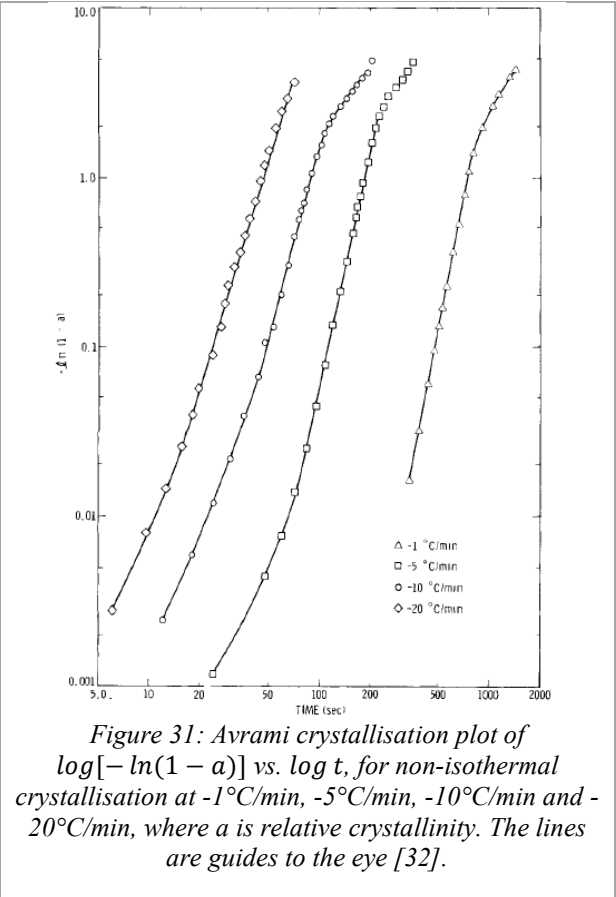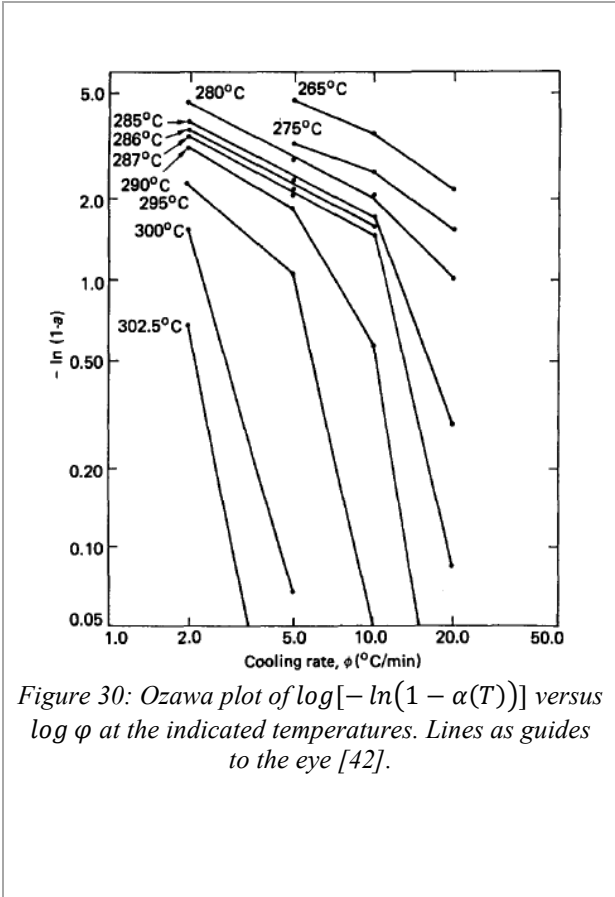
$$\alpha(T) = 1 - \exp\left(-\frac{K^*(T)}{\varphi^m}\right) \tag{4.14}$$

where $K^*(T)$ is a heating/cooling function dependent on temperature, φ represents the cooling rate, and m is assumed to be constant and independent of temperature. The crystallisation in this model is dependent on temperature, and therefore relies on crystallinity sampling at different temperatures during crystallisation at different cooling rates. If a crystallisation process is correctly modelled by Ozawa analysis, a plot of $\log[-\ln(1 - \alpha(T))]$ against $\log \varphi$ would result in a series of parallel lines with slope m and intercept K^* [42,79,80].

The aforementioned models have the same limitation as the Avrami model as they cannot model dual crystallisation behaviour, and are therefore not ideal for modelling PEKK or other PAEKs, where secondary crystallisation is significant [32,40,42,79,81,82]. This is obvious in Cebe and Hong's [42] attempt to use the Ozawa and Avrami equations to model non-isothermal crystallisation of unreinforced PEEK with cooling rates between 2 and 20°/min, shown in Figure 30. With the Ozawa model, they obtained a distinct curvature in their results, likely due to the inaccurate assumption in the model that the constants are independent of temperature. With Avrami fitting, they found that for low degrees of conversion up to 0.20, the model was linear for the entire range of cooling rates applied. This therefore implies that it is after this relative crystallinity is obtained that secondary crystallisation starts taking

place – Cebe and Hong stated this happens within the range of 0.24-0.35 at the faster rates used in their study. It is worth noting that the meaning that the Avrami exponent *n* holds during isothermal crystallisation is lost in this case and is not representative of crystallisation morphology.

In a later study, Cebe [32] implemented the same Avrami equation on CF/PEEK when undergoing various cooling rates, and found the data to be linear over a very wide range of degrees of conversion. While it is likely that there exist molecular weight differences between Cebe's [32] and Cebe and Hong's [42] studies, linear ranges can be observed in the range of 0.1-0.8 in cooling rates between 1 and 20°C/min in Figure 31. Departures from linearity at the beginning and end of the crystallisation process are explained as an exaggeration of small errors in the assignment of the crystallisation starting time, and as a switch between primary and secondary crystallisation respectively. It is observed that in comparison to neat PEEK crystallisation, crystallisation initiates and peaks at higher temperatures (implying faster kinetics) in the composite. While this may be due to molecular weight differences, it is also possible that the carbon fibres act as sites for nucleation and transcrystalline growth, as discussed in previous sections.

Figure 30: Ozawa plot of $log[-ln(1 - \alpha(T))]$ versus $log\,\varphi$ at the indicated temperatures. Lines as guides to the eye [42].

Figure 31: Avrami crystallisation plot of $log[-ln(1 - a)]$ vs. $log\,t$, for non-isothermal crystallisation at -1°C/min, -5°C/min, -10°C/min and -20°C/min, where a is relative crystallinity. The lines are guides to the eye [32].

Velisaris and Seferis [34] extended their model (discussed in Section 4.1) to the non-isothermal case on PEEK by utilising an integral Avrami expression. Each crystallisation rate process *i* is modelled as follows:

$$\alpha_i(t) = 1 - \exp\left[-\int_0^t k(T)_i n_i t^{n_i - 1}\, dt\right] \tag{4.15}$$

where the crystallisation rate $k(T)_i$ is now temperature-dependent. Extended for a dual crystallisation mechanism ($i = 1, 2$), this becomes:

$$\alpha(t) = w_1\left[1 - \exp\left[-\int_0^t k(T)_1 n_1 t^{n_1-1}\ dt\right]\right] + w_2\left[1 - \exp\left[-\int_0^t k(T)_2 n_2 t^{n_2-1}\ dt\right]\right] \quad (4.16)$$

It is worth noting that in these authors' work [34], $\alpha(t)$ is printed as $X_{vc}X_{vc\infty}$, where X_{vc} is the volume fraction crystallinity and $X_{vc\infty}$ is the equilibrium volume fraction crystallinity. Other authors that use this model [33,83] define $\alpha(t)$ as $X_{vc}/X_{vc\infty}$, following the commonly used definition of relative volume fraction crystallinity. Further explanation of this model can be found in the Velisaris and Seferis' paper [34].

Applying this model on neat PEEK, they obtained the best model with $n_1 = 2.5$ and $n_2 = 1.5$, as per their isothermal modelling. The results show a good correspondence with experimental values, with perhaps a slight deviation from experimental results towards the end of the crystallisation process, as shown in Figure 32 below; however, as discussed previously, the neat and composite samples contain different grades of PEEK, and therefore achieved volume fraction crystallinities and kinetics are not comparable.
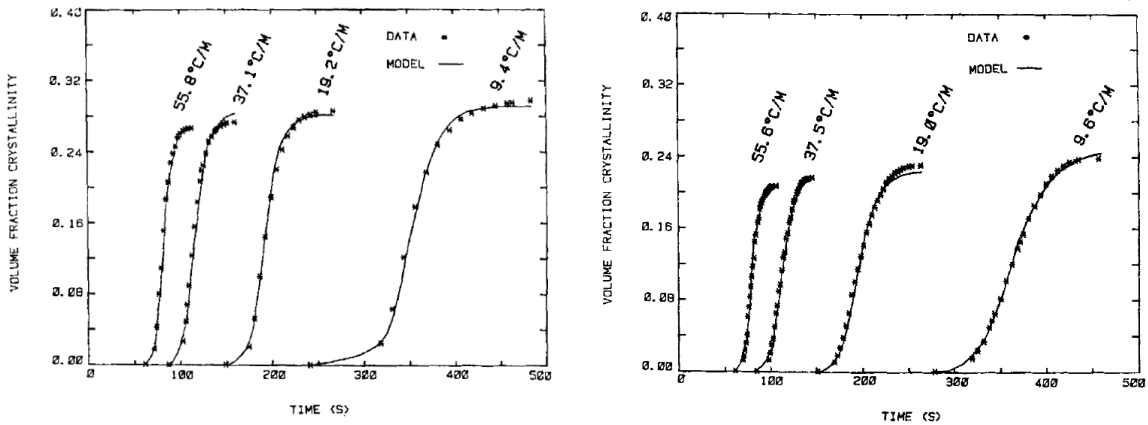

Figure 32: Volume fraction crystallinity versus time for the non-isothermal crystallisation of (a) neat PEEK resin and (b) PEEK resin in APC2 at various cooling rates. Lines represent predictions obtained by fitting the data to the parallel model, with best fit dynamic parameters [34].

Choupin [31] developed a non-isothermal model in their thesis work which takes into account this dual crystallisation and is applicable for any thermoplastic. The model is not reliant on material-specific parameters, and was applied to neat PEKK 60/40 and 70/30. The work is based on the models proposed by Hillier [53] and Patel and Spruiell [78], and considers non-isothermal crystallisation cycles as a succession of brief isotherms. This allows for the addition of the relative crystallinity formed during each small isotherm, in order to determine the crystallinity obtained for the entire non-isothermal crystallisation. The derivation of the model can be found in Choupin's work [31], where its final form is as follows:

$$\frac{d\alpha(t)}{dt} = w_1 n_1 k_1^{\frac{1}{n_1}}\left[-\ln\left(1 - a_1(t)\right)\right]^{\frac{n_1-1}{n_1}}[1 - \alpha_1(t)] + w_2 k_2[\alpha_1(t) - \alpha_2(t)] \quad (4.17)$$

This model tends to over-predict crystallisation kinetics, due to not accounting for an induction time for nucleation. Choupin argued that this phenomenon is due to the assumption that nucleation and growth kinetics are proportional, which may not be true for non-isothermal crystallisation.

Another model worth mentioning which takes a different approach to dual crystallisation modelling is the following one developed by Tobin [84–86]. Tobin argued that the Avrami equation is not suitable for crystallisation modelling of any polymer, as it assumes the system to be completely melted with no residual nuclei, only obtaining adequate fits below 10-30% conversion. They proposed models for heterogeneous and homogeneous nucleation, as well as a mixed-mode model which simply consists of a linear combination of the first two expressions:

$$\frac{\alpha(t)}{1 - \alpha(t)} = kNt^n + KI^* \int_0^\tau (t - \tau)^n [1 - \alpha(\tau)] d\tau \tag{4.18}$$

where $\alpha(t)$ is the relative crystallinity at time t, k is a constant containing nucleation and growth parameters, n is an integer similar to the Avrami exponent, the value of which depends on the nucleation mechanism and the crystal growth form; N is the initial number of heterogeneous nuclei and I^* is the rate of homogeneous nucleation. The first term, kNt^n, represents heterogeneous nucleation and growth, and the integral term corresponds to homogeneous nucleation and growth.

Choe and Lee [87] applied this model to unreinforced PEEK in later work, therefore taking a different approach to other authors studying this polymer: instead of considering a primary and secondary crystallisation mode, nucleation type (heterogeneous or homogeneous) is considered. They adapted the Tobin equation to non-isothermal modelling by transforming it to differential form and verified the model again with a range of cooling rates 2-50°C/min. Details of this can be found in their work.

It was found that at slow cooling rates, where the material is exposed at the higher temperatures for longer, heterogeneous growth dominates, and using only the first term of the equation kNt^n was suitable, obtaining very high correlations as shown in Figure 33. Homogeneous nucleation does not occur in this case because the free energy of nuclei formation is very high, and instead growth processes dominate crystallisation. At higher cooling rates, on the other hand, using only the heterogeneous term kNt^n resulted in a poor fit, as per Figure 34. This is because the two processes are present, and when using a contribution of both heterogeneous and homogeneous nucleation processes in the model, a good correlation was obtained.
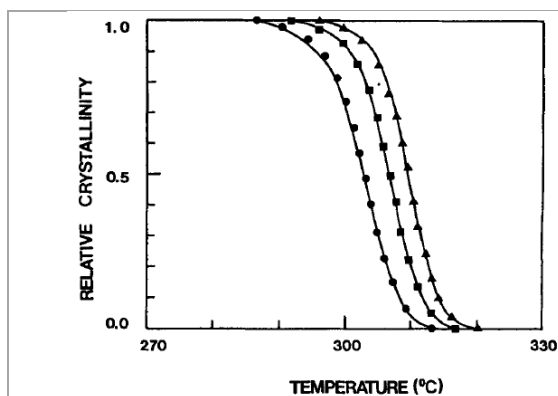
Figure 33: Comparison of the experimental data (points) with the calculated values (lines) from using only the heterogeneous term kNt^n in Eqn. (4.18) at the cooling rates (●) 5°C/min, (■) 3°C/min, and (▲) 2°C/min [87].
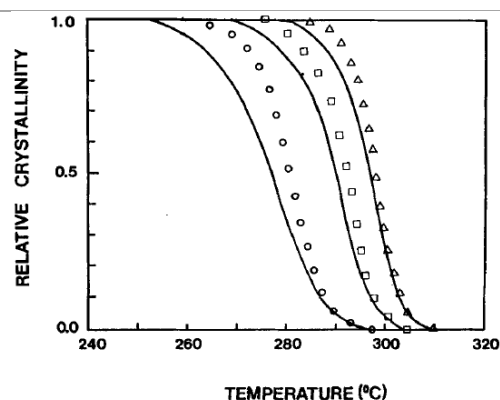

Figure 34: Comparison of the experimental data (points) with the calculated values (lines) from using only the heterogeneous term kNt^n in Eqn. (4.18) at the cooling rates (○) 50°C/min, (□) 20°C/min, and (Δ) 10°C/min [87].

To the knowledge of the authors, this model has not been used as extensively as the Avrami model and subsequent models based on it. A reason for this may be that, while the presence of heterogeneity and homogeneity is a valid argument, primary and secondary crystallisation have been proven to be the key processes taking place in PEEK and PEKK, and cannot be disregarded. As the majority, if not all, of these models have been implemented on experimental data obtained via DSC, where a small amount of material is held in the melt and therefore it is likely that there are no residual nuclei, this may contribute to the fact that the Avrami-based models effectively fit results. Implementing Tobin's model on composite systems may result in different approaches, as carbon fibres have been shown to act as nucleation sites at times; or possibly obtaining experimental results from samples with a variety of residual nuclei would result in different outcomes for all of the above models.

Overall, the investigation into the crystallisation kinetics of unreinforced PEEK and PEKK under non-isothermal conditions is not particularly conclusive or recent (with the exception of Choupin's work from 2017 [31], which is part of a doctoral thesis), and no particular model has been widely used in literature. This is likely due to a lack of understanding around kinetics under isothermal conditions to begin with, until perhaps more recently. Evaluation of non-isothermal crystallisation kinetics of composite systems is even sparser, potentially due to the same reasons. A better understanding of isothermal conditions is necessary prior to developing accurate models under non-isothermal conditions.

4.3.   Modelling of Transcrystallinity

Existing modelling of transcrystallinity is seen to take a different approach to the rest of this section, as it does not only depend on thermal conditions, but also on the fibre in question, as previously discussed. The effect of the fibre type on crystallisation kinetics can be one of three: speed up, slow down, or none. Some authors maintain that the presence of a transcrystalline region lowers the Avrami exponent, due to the one-dimensional growth occurring at the fibre surface instead of three-dimensional spherulitic growth, as discussed in Section 4.1.

Apart from this, there is no further mention of any potential impact that the presence of a transcrystalline phase may have on the aforementioned crystallisation kinetics models. There is little literature focusing on the kinetics of transcrystalline growth and its modelling on PEKK or PEEK, one of these being Chelaghma et al. [88] with a pixel colouring technique, a method previously studied and implemented by Ruan et al. [89–91] in a neat matrix system and with short carbon fibre inclusions. Here, crystalline nuclei are randomly dispersed and identified by a colour, which grow in a spherulitic manner at a constant radial speed until different spherulites come into contact, causing impingement and therefore stopping further growth. Nucleation and growth rates were determined by previous microscopic analysis. Three different models were created, making the following assumptions:

- Model 1: Fibres with entire surfaces acting as nucleation sites.
- Model 2: Fibres with nucleation sites on surfaces matching microscopy results (only parts of the fibre acted as nucleation sites – shown in Figure 35 and Figure 36).
- Model 3: Fibre surfaces that had no effect on the matrix's nucleation.

These proved to be a good method to model primary crystallisation of PEKK, confirming that fibres whose surfaces act as nucleation sites accelerate the overall crystallisation process, causing the formation of a transcrystalline zone. A kinetics comparison between these and the empirical results was performed, showing that model 2 had the best fit, which only develops transcrystallinity on zones observed to do so.
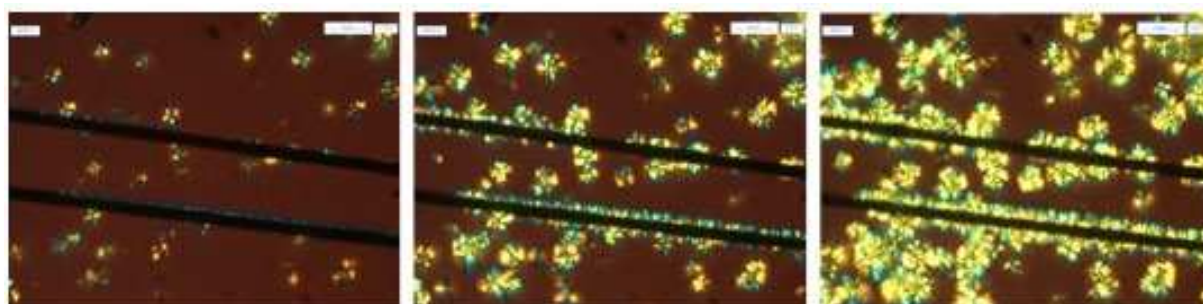

Figure 35: Optical micrograph observation of the transcrystalline phase of CF/PEKK at 320°C isotherm [88].
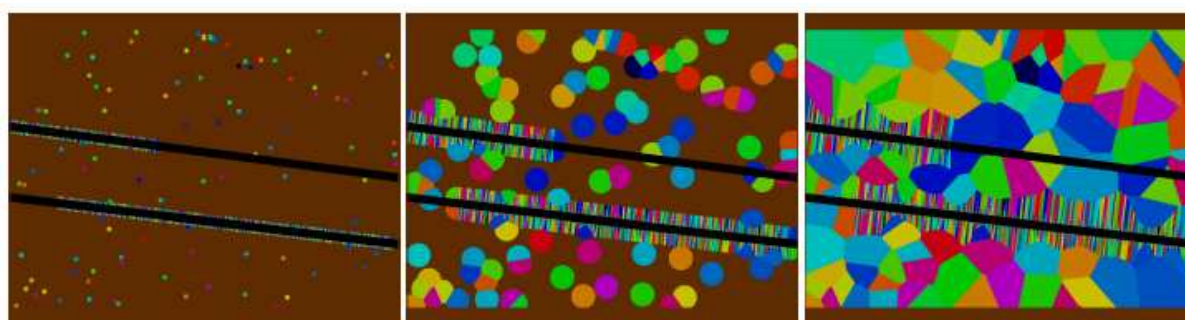

Figure 36: Pixel colouring simulation of a polymeric film in the presence of two carbon fibres after locating nucleation sites as per the identified zones in optical micrographs [88].

There are still some elements that remain to be integrated into the above model, in order for this to be realistic. Secondary crystallisation is not included in this model, likely due to the difficulty in observing this phenomenon taking place the same way that spherulitic growth does. The author also points out the

40

assumption of temperature homogeneity across the sample, which may have not been the case; as well as the thermal contribution linked to crystallisation being ignored [88].

Another composite modelling approach worth mentioning is that presented by Guan and Pitchumani [92], which focused on the tow-placement process of CF/PEEK. This model does take into account spatial temperature variation and thermal history (as a consequence of the manufacturing process' heat source). The model domain focuses on a small area located at one of the interfaces between substrate prepreg layers, bounded at the top and bottom by neighbouring fibres, as shown in Figure 37. Further details of the model, as well as the heat transfer boundary conditions and further mathematical details of the analysis, can be found in [92,93].
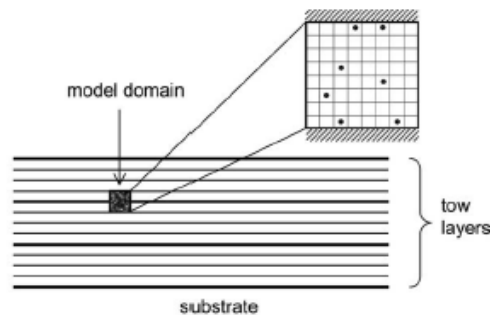

Figure 37: Illustration of a location substrate where the microstructural modelling is considered [92].

Studied parameters were based on using a hot gas torch as a heating source: incidence angle, torch exit diameter, torch distance to the target, hot gas temperature, gas velocity, line speed, and number of layers in the tow substrate. The discussion of the results is lengthy and focuses on optimising the manufacturing process, which lies outside of the scope of this literature review. The model, however, effectively shows the dependence of transcrystallinity on the different processing parameters, and demonstrates a larger development of this phase with longer exposure times. The model follows the impact that nucleation density in the bulk has: with a lower nucleation density, the longer the transcrystalline region is allowed to grow. This correlates with larger spherulite sizes in the bulk, since there are fewer nucleation sites and therefore spherulites grow for longer before they reach impingement. A figure comparing two simulations with extreme processing conditions, showing the largest and smallest spherulites and transcrystallinity development in CF/PEEK can be seen in Figure 38, including snapshots at different relative crystallinities.

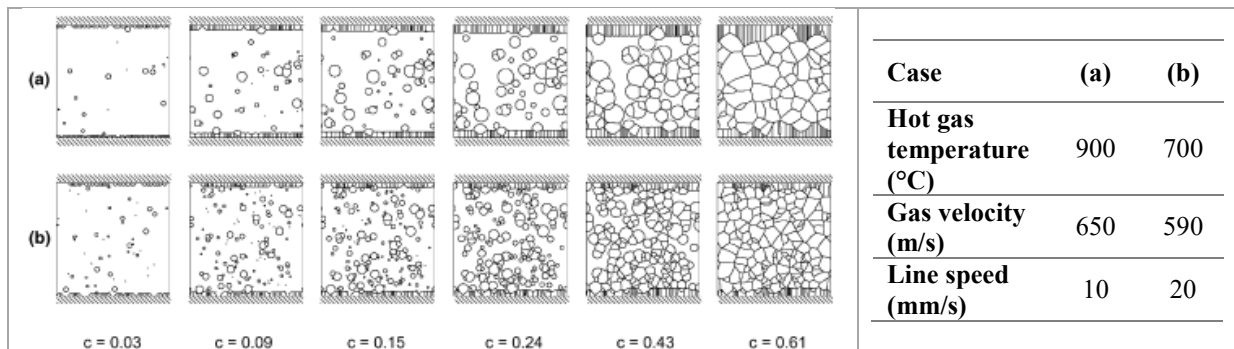| Case	(a)	(b)
Hot gas temperature (°C)	900	700
Gas velocity (m/s)	650	590
Line speed (mm/s)	10	20

Figure 38: Comparison of spherulitic microstructure observations obtained from simulation between two extreme processing conditions at different relative crystallinities "c". For both cases, incidence angle is 60°, torch exit diameter is 8mm, and torch distance to target is 32mm [92].

Results show that various spherulitic morphologies can be achieved with different processing conditions that will produce the same overall degree of crystallinity, and therefore processing parameters can be optimised in order to achieve the desired mechanical properties. The model focuses, however, on a small segment of the composite during the manufacturing process, not considering other factors such as degradation, interlaminar surface contact or bonding. Experimental verification of the authors' findings would provide further grounds for the success of this model.

5. Future Directions

While there seems to be an established understanding of PEKK's morphology, structure and crystallisation behaviour, research on the impact of carbon fibre reinforcement in PEKK is much less conclusive. As has been reported in this review, it is clear that the nature of the fibre surface can have an effect on the crystallisation on the surface. It is difficult, however, to understand transcrystallinity and to correlate its presence (or lack thereof) across different fibres without an understanding of the similarities and differences between said fibres and their surfaces. This is something that is not thoroughly reported in the literature assessing the effect of transcrystallinity in CF/PEEK and CF/PEKK, and leads to confusion. The fibre type, modulus and surface finish can all play a role in the surface energy and will therefore influence the presence of transcrystallinity.

Furthermore, reporting on the mechanical behaviour of the transcrystalline phase is also inconclusive. Some literature shows that the presence of a transcrystalline phase results in better mechanical performance, improved fibre-matrix adhesion and higher load transfer, while other authors describe the opposite. Further investigations to clarify this is important, particularly with PEKK, where these studies are sparse.

Once the understanding of transcrystallinity in unreinforced PEEK and PEKK is better developed, then kinetics modelling may develop further into their fibre-reinforced composites. Current models used for unreinforced PEKK need to be further verified and then adapted to the composite counterparts. Transcrystallinity simulations, even though sparse, have proved to be successful [88,92]. It will be interesting to see further implementation of this modelling, or new models that can lead to new findings and investigations on the kinetics of neat and composite PEKK.

Finally, and perhaps the largest challenge to overcome, is the meaning and applicability of this research to industry. Studies covered in this review focus on small scale morphology and properties, developed and evaluated under highly controlled conditions. An example of this is the DSC, where samples weighing between 5-20mg undergo a controlled thermal cycle in an inert environment.

While it is paramount to develop an understanding of the material behaviour performing small scale in-lab tests, these are far from emulating the conditions of real-life manufacturing, where thick composite sections and a variety of manufacturing techniques may cause thermal gradients, exposure to high heating and cooling rates, and even thermal degradation due to exposure to more reactive environments. It is therefore key to correlate lab-scale studies to industrial manufacturing scenarios and performance. An in-depth understanding of the relationship between manufacturing, crystallinity development and the final mechanical properties will help to improve the reliability and paths to certification of thermoplastic

composite structures in high-performing industrial applications which are currently dominated by epoxy composites. Press and autoclave manufacturing, for example, offer controlled cooling conditions even at a large industrial scale (less controlled than the DSC - due to the size of the equipment, metal moulds and the manufactured parts). Automated higher-speed, out-of-autoclave manufacturing techniques are of increasing interest, driven by the need to eliminate the high capital cost of autoclaves and the bottlenecks caused, as well as any post-processing techniques that increase the cost of manufacturing these parts. An example of this is Automated Tape Placement (ATP), an automated process where prepreg tape is laid down on a metal tool, consolidated onto previously laid tape with the help of a heat source and a consolidation roller. Due to the nature of ATP, prepreg undergoes a very fast heating and uncontrolled cooling process, and therefore crystallinity can vary across the laminate thickness, a schematic of which is shown in Figure 39. The figure outlines the crystallinity distribution uncertainty in the resulting laminate from ATP, and the current need of post-processing in order to obtain a uniformed and controlled crystallinity.
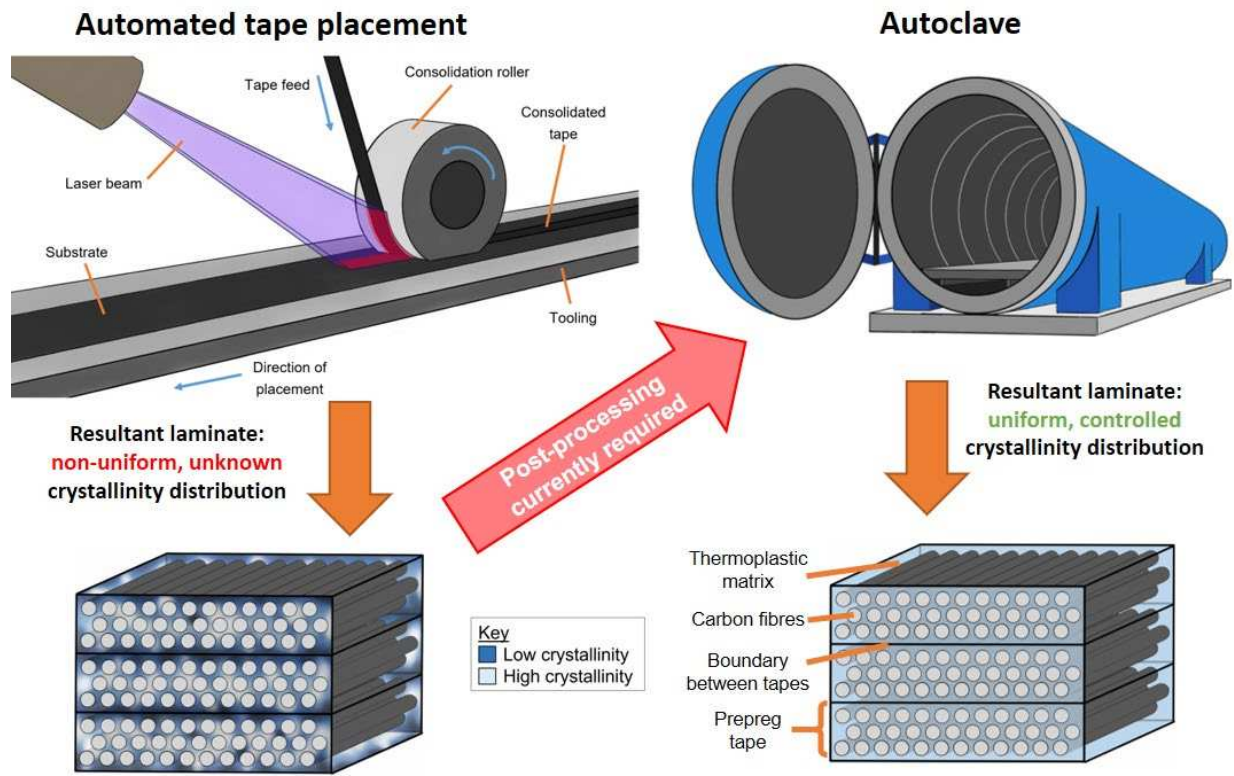

Figure 39: Schematic of a laminate consolidated by Automated Tape Placement (left) and autoclave (right). Different shades of blue show crystallinity variation within the matrix. ATP schematic drawn after [13].

This is not a challenge only applicable to PEKK, but to any semicrystalline thermoplastic matrix composite consolidated by ATP [94]. There are several studies available on CF/PEEK in ATP-manufactured laminates focusing on mechanical characterisation and consolidation quality [13,15,70,95–99], and fewer in the case of CF/PEKK [97], however literature covering variation in crystallinity specifically is sparse [16]. Therefore, studies on samples extracted from processes like ATP would be key in understanding how CF/PEKK composites behave, and their applicability in high-performance applications.

Another manufacturing challenge is the introduction of PEKK and short CF/PEKK composites to 3D printing. This is an additive manufacturing technique which deposits molten polymer to create a three-dimensional object. This exposes the material to uncontrolled cooling rates without any consolidation pressure, which may result in uneven interlayer bonding, crystallinity gradients and anisotropic mechanical properties if the processing conditions and their impact on the printing material are not well understood. 3D-printed composite forms of PEKK and other PAEKs are also attractive in similar high-performance applications as ATP, such as aerospace, automotive or off-shore oil and gas exploration [100], but unreinforced PAEKs are particularly interesting in medical applications, due to their biocompatibility, chemical resistance and antibacterial properties, as well as possessing similar mechanical properties to human bones [101–103].

While some studies on crystallinity are available for PEEK and other PAEKs [104,105], research on PEKK and CF/PEKK 3D printing covers the impact of infill density, topology and T/I ratio on mechanical performance [100,101,106], with no mention of the effect of the printing process on crystallinity. Namely, an understanding of the impact of nozzle temperature on the polymer melting, crystallisation and interface between printing layers is necessary, as well as the influence of nozzle size and deposition speeds on cooling rates, and any potential need and effect of post-processing, in order to establish a good understanding of PEKK's behaviour in 3D printing.

6. Conclusions

An understanding of the crystallinity development in CF/PEKK composites is important to establish the reliability of such products in high-performance applications such as the aerospace or the oil and gas sector. There are studies on the crystalline morphology of PEKK, its terephthalic/isophthalic content ratios and its influence on crystallisation. The external factors that affect crystallisation are also clearly identified, such as crystallisation mode and thermal history, and their effects on the unit cell and spherulite morphology.

The effect of carbon fibre reinforcement on the crystallisation morphology of PEKK at the fibre-matrix interface is not as obvious as crystallisation in the bulk. Literature covering this is sparse, so a comparison with PEEK has been drawn whenever relevant. Overall, the presence of transcrystallinity is still a topic under investigation and different observations have been reported. There is a likely dependence on the fibre surface energy, where a low surface energy results in little attraction between the fibre and matrix and therefore lamellae form perpendicular to the surface, creating a transcrystalline phase of epitaxial form; whereas high-energy surfaces invite lamellae to grow flat-on, and therefore growths take on a more spherulitic shape and no transcrystallinity is formed. Transcrystalline growth is also observed to be incentivised by high isothermal temperatures and slow cooling rates, which allows for larger crystallisation growth from the fibre surface and less nucleation in the bulk. Simulations have been developed that successfully demonstrate the development of this phase. Literature reports different findings, however, when assessing whether the presence of transcrystallinity benefits or hinders composite mechanical properties. Further investigations on different carbon fibre types and their interactions with PEKK polymers are needed in order to reach a consensus on this topic.

A dual crystallisation mode is reported for PEKK in both unreinforced and carbon fibre reinforced composite form, consisting of a primary, spherulitic growth followed by a secondary stage, where interlamellar crystalline structures grow. Quantifying the primary and secondary crystalline phases present has been the object of study particularly when modelling crystallisation kinetics, mainly in the case of unreinforced PEKK. The impact of thermal processing cycles on this is clearly reported, where holding temperature and time are observed to influence the extent and nature of crystallinity developed in the material. Robust models have been developed for the isothermal crystallisation cases of PEKK, but further refinement is needed in the case of non-isothermal crystallisation kinetics.

In the case of CF/PEKK composites, crystallisation kinetics studies are minimal. The available literature reports higher isothermal temperatures resulting in faster kinetics for the composites, potentially due to fibres acting as nucleation sites and kinetics in the bulk being low; whereas at lower isothermal temperatures the difference is not notable, since nucleation in the bulk is faster and fibres hinder macromolecular chain mobility. A few of the aforementioned crystallisation kinetics models applied to unreinforced PEEK and PEKK have also been implemented to their composite counterparts with some success, however, once again this is less diligent than for neat PEEK and PEKK, and existing models may need some adaptation to account for the inclusion of carbon fibres.

Acknowledgements

Bibliography

[1] Blundell DJ, Crick RA, Fife B, Peacock J, Keller A, Waddon A. Spherulitic morphology of the matrix of thermoplastic PEEK/carbon fibre aromatic polymer composites. J Mater Sci 1989;24:2057–64. https://doi.org/10.1007/BF02385421.

[2] Choupin T, Fayolle B, Régnier G, Paris C, Cinquin J, Brulé B. Isothermal crystallization kinetic modeling of poly(etherketoneketone) (PEKK) copolymer. Polymer 2017;111:73–82. https://doi.org/10.1016/j.polymer.2017.01.033.

[3] Mazur RL, Oliveira PC, Rezende MC, Botelho EC. Environmental effects on viscoelastic behavior of carbon fiber/PEKK thermoplastic composites. J Reinf Plast Compos 2014;33:749–57. https://doi.org/10.1177/0731684413515955.

[4] Hassan EAM, Ge D, Yang L, Zhou J, Liu M, Yu M, et al. Highly boosting the interlaminar shear strength of CF/PEEK composites via introduction of PEKK onto activated CF. Compos Part Appl Sci Manuf 2018;112:155–60. https://doi.org/10.1016/j.compositesa.2018.05.029.

[5] Quiroga Cortés L, Caussé N, Dantras E, Lonjon A, Lacabanne C. Morphology and dynamical mechanical properties of poly ether ketone ketone (PEKK) with meta phenyl links. J Appl Polym Sci 2016;133:1–10. https://doi.org/10.1002/app.43396.

[6] Reitman M, Jaekel D, Siskey R, Kurtz SM. Morphology and Crystalline Architecture of Polyaryletherketones. 2nd ed. Elsevier Inc.; 2012. https://doi.org/10.1016/B978-1-4377-4463-7.10004-1.

[7] Donadei V, Lionetto F, Wielandt M, Offringa A, Maffezzoli A. Effects of blank quality on press-formed PEEK/Carbon composite parts. Materials 2018;11. https://doi.org/10.3390/ma11071063.

[8] Cheng SZD, Ho RM, Hsiao BS, Gardner KH. Polymorphism and crystal structure identification in poly(aryl ether ketone ketone)s. Macromolecules 1996;197:185–213.

[9]   Deignan A, Stanley WF, McCarthy M. Insights into wide variations in carbon fibre/polyetheretherketone rheology data under automated tape placement processing conditions. J Compos Mater 2018;52:2213–28. https://doi.org/10.1177/0021998317740733.

[10] Gardner KH, Hsiao BS, Faron KL. Polymorphism in poly (aryl ether ketone). Polymer 1994;35:2290–5.

[11] Jin L, Ball J, Bremner T, Sue HJ. Crystallization behavior and morphological characterization of poly(ether ether ketone). Polymer 2014;55:5255–65. https://doi.org/10.1016/j.polymer.2014.08.045.

[12] Rodríguez-Lence F, Zuazo M, Calvo S, Lorenzo E. Activities on in-situ consolidation by automated placement technologies. 16th Eur Conf Compos Mater 2014:22–6.

[13] Stokes-Griffin CM, Compston P. The effect of processing temperature and placement rate on the short beam strength of carbon fibre-PEEK manufactured using a laser tape placement process. Compos Part Appl Sci Manuf 2015;78:274–83. https://doi.org/10.1016/j.compositesa.2015.08.008.

[14] Zhu K, Tan H, Wang Y, Liu C, Ma X, Wang J, et al. Crystallization and mechanical properties of continuous carbon fiber reinforced polyether-ether-ketone composites. Fibers Polym 2019;20:839–46. https://doi.org/10.1007/s12221-019-8791-5.

[15] Kilroy JP, Ó Brádaigh CM, Semprimoschnig COA. Mechanical and physical evaluation of a new carbon fibre/PEEK composite system for space applications. SAMPE J 2008:1–12.

[16] Esguerra-Arce I, Martín MI, Pérez-Pastor A, García-Martínez V. Evolution of crystallinity with multiple lamination steps in high performance thermoplastic composites by in-situ consolidation process (non-peer reviewed). Twenty-Second Int Conf Compos Mater 2019.

[17] Gardner KCH, Hsiao BS, Matheson RR, Wood BA. Structure, crystallization and morphology of poly (aryl ether ketone ketone). Polymer 1992;33:2483–95. https://doi.org/10.1016/0032-3861(92)91128-O.

[18] Ho RM, Cheng SZD, Hsiao BS, Gardner KH. Crystal morphology and phase identifications in poly(aryl ether ketone)s and their copolymers. 3. Polymorphism in a polymer containing alternated terephthalic acid and isophthalic acid isomers. Macromolecules 1995;28:1938–45. https://doi.org/10.1021/ma00110a030.

[19] Hsiao BS, Chang IY, Sauer BB. Isothermal crystallization kinetics of poly(ether ketone ketone) and its carbon-fibre-reinforced composites. Polymer 1991;32:2799–805. https://doi.org/10.1016/0032-3861(91)90111-U.

[20] Choupin T, Fayolle B, Régnier G, Paris C, Cinquin J, Brulé B. A more reliable DSC-based methodology to study crystallization kinetics: Application to poly(ether ketone ketone) (PEKK) copolymers. Polymer 2018;155:109–15. https://doi.org/10.1016/j.polymer.2018.08.060.

[21] Gao S-L, Kim J-K. Cooling rate influences in carbon fibre/PEEK composites. Part 1. Crystallinity and interface adhesion. Compos Part Appl Sci Manuf 2000;31:517–30. https://doi.org/10.1016/S1359-835X(00)00009-9.

[22] Harris L. A study of the crystallisation kinetics on PEEK and PEEK composites. University of Birmingham, 2011.

[23] Cogswell FN. Thermoplastic matrix resins: Polyetheretherketone. Thermoplast. Aromat. Polym. Compos. Study Struct. Process. Prop. Carbon Fibre Reinf. Polyetheretherketone Relat. Mater., Butterworth-Heinemann Ltd; 1992, p. 21–30.

[24] Hsiao BS, Gardner KH, Cheng SZD. Crystallization of poly(aryl ether ketone ketone) copolymers containing terephthalate/isophthalate moieties. J Polym Sci Part B Polym Phys 1994;32:2585–94. https://doi.org/10.1002/polb.1994.090321604.

[25] Arkema. Introduction to ultra high-performance Kepstan® PEKK 2020.

[26] Blundell DJ, Newton AB. Variations in the crystal lattice of PEEK and related para-substituted aromatic polymers: 2. Effect of sequence and proportion of ether and ketone links. Polymer 1991;32:308–13. https://doi.org/10.1016/0032-3861(91)90019-F.

[27] Ho RM, Cheng SZD, Hsiao BS, Gardner KH. Crystal Morphology and Phase Identifications in Poly(aryl ether ketone)s and Their Copolymers. 1. Polymorphism in PEKK. Macromolecules 1994;27:2136–40. https://doi.org/10.1021/ma00086a023.

[28] Painter PC, Coleman MM. Polymer Morphology. Fundam. Polym. Sci. Introd. Text. 2nd edition, Routledge; 1997, p. 250–3.

[29] Lee Y, Porter RS. Crystallization of poly(etheretherketone) (PEEK) in carbon fiber composites. Polym Eng Sci 1986;26:633–9. https://doi.org/10.1002/pen.760260909.

[30] Chen EJH, Hsiao BS. The effects of transcrystalline interphase in advanced polymer composites. Polym Eng Sci 1992;32:280–6. https://doi.org/10.1002/pen.760320408.

[31] Choupin T. Mechanical performances of PEKK thermoplastic composites linked to their processing parameters. École nationale supérieure d'arts et métiers, 2017.

[32] Cebe P. Non-isothermal crystallization of poly(etheretherketone) aromatic polymer composite. Polym Compos 1988;9:271–9. https://doi.org/10.1002/pc.750090405.

[33] Cebe P. Application of the parallel Avrami model to crystallization of poly(etheretherketone). Polym Eng Sci 1988;28:1192–7. https://doi.org/10.1002/pen.760281809.

[34] Velisaris CN, Seferis JC. Crystallization kinetics of polyetheretherketone (peek) matrices. Polym Eng Sci 1986;26:1574–81. https://doi.org/10.1002/pen.760262208.

[35] Waddon AJ, Hill MJ, Keller A, Blundell DJ. On the crystal texture of linear polyaryls (PEEK, PEK and PPS). J Mater Sci 1987;22:1773–84. https://doi.org/10.1007/BF01132406.

[36] Lustiger A. Morphological aspects of the interface in the PEEK-carbon fiber system. Polym Compos 1992;13:408–12. https://doi.org/10.1002/pc.750130511.

[37] Hobbs SY. Row nucleation of isotactic polypropylene on graphite fibres. Nat Phys Sci 1971;234. https://doi.org/10.1038/physci234012a0.

[38] Chang IY, Hsiao BS. Thermal properties of high performance thermoplastic composites based on poly(ether ketone ketone) (PEKK). 36th Int SAMPE Symp 1991:1587–601.

[39] Bassett DC, Olley RH, Al Raheil IAM. On crystallization phenomena in PEEK. Polymer 1988;29:1745–54. https://doi.org/10.1016/0032-3861(88)90386-2.

[40] Bessard E, De Almeida O, Bernhart G. Unified isothermal and non-isothermal modelling of neat PEEK crystallization. J Therm Anal Calorim 2014;115:1669–78. https://doi.org/10.1007/s10973-013-3308-8.

[41] Blundell DJ, Osborn BN. The morphology of poly(aryl-ether-ether-ketone). Polymer 1983;24:953–8. https://doi.org/10.1016/0032-3861(83)90144-1.

[42] Cebe P, Hong S-D. Crystallization behaviour of poly(ether-ether-ketone). Polymer 1986;27:1183–92. https://doi.org/10.1016/0032-3861(86)90006-6.

[43] Cheng SZD, Cao MY, Wunderlich B. Glass transition and melting behavior of poly(oxy-1,4-phenyleneoxy-1,4-phenylenecarbonyl-1,4-phenylene) (PEEK). Macromolecules 1986;19:1868–76. https://doi.org/10.1021/ma00161a015.

[44] Ko TY, Woo EM. Changes and distribution of lamellae in the spherulites of poly(ether ether ketone) upon stepwise crystallization. Polymer 1996;37:1167–75. https://doi.org/10.1016/0032-3861(96)80843-3.

[45] Lattimer MP, Hobbs JK, Hill MJ, Barham PJ. On the origin of the multiple endotherms in PEEK. Polymer 1992;33:3971–3. https://doi.org/10.1016/0032-3861(92)90391-9.

[46] Lee Y, Porter RS, Lin JS. On the double-melting behavior of poly(ether ether ketone). Macromolecules 1989;22:1756–60. https://doi.org/10.1021/ma00194a043.

[47] Medellín-Rodríguez FJ, Phillips PJ. Bulk crystallization of poly(aryl ether ether ketone) (PEEK). Polym Eng Sci 1996;36:703–12. https://doi.org/10.1002/pen.10457.

[48] Tan S, Su A, Luo J, Zhou E. Crystallization kinetics of poly(ether ether ketone) (PEEK) from its metastable melt. Polymer 1999;40:1223–31. https://doi.org/10.1016/S0032-3861(98)00275-4.

[49] Tardif X, Pignon B, Boyard N, Schmelzer JWP, Sobotka V, Delaunay D, et al. Experimental study of crystallization of PolyEtherEtherKetone (PEEK) over a large temperature range using a nano-calorimeter. Polym Test 2014;36:10–9. https://doi.org/10.1016/j.polymertesting.2014.03.013.

[50] Verma RK, Hsiao BS. Some new insights into the crystallization and melting mechanism in semicrystalline semistiff polymers. Trends Polym Sci 1996;9:312–9.

[51] Wei C-L, Chen M, Yu F-E. Temperature modulated DSC and DSC studies on the origin of double melting peaks in poly(ether ether ketone). Polymer 2003;44:8185–93. https://doi.org/10.1016/j.polymer.2003.10.009.

[52] Zhang Z, Zeng H. Effects of thermal treatment on poly(ether ether ketone). Polymer 1993;34:3648–52. https://doi.org/10.1016/0032-3861(93)90049-G.

[53] Hillier IH. Modified avrami equation for the bulk crystallization kinetics of spherulitic polymers. J Polym Sci A 1965;3:3067–78. https://doi.org/10.1002/pol.1965.100030902.

[54] Yuan M, Galloway JA, Hoffman RJ, Bhatt S. Influence of molecular weight on rheological, thermal, and mechanical properties of PEEK. Polym Eng Sci 2011;51:94–102. https://doi.org/10.1002/pen.21785.

[55] Tung CM, Dynes PJ. Morphological characterization of polyetheretherketone–carbon fiber composites. J Appl Polym Sci 1987;33:505–20. https://doi.org/10.1002/app.1987.070330218.

[56] Gao S-L, Kim J-K. Crystallinity and interphase properties of carbon fibre/PEEK matrix composites. ICCM12 Conf Paris Fr 1999.

[57] Ye L, Scheuring T, Friedrich K. Matrix morphology and fibre pull-out strength of T700/PPS and T700/PET thermoplastic composites. J Mater Sci 1995;30:4761–9. https://doi.org/10.1007/BF01154482.

[58] Zou YL, Netravali AN. Ethylene/ammonia plasma polymer deposition for controlled adhesion of graphite fibers to PEEK. J Adhes Sci Technol 1995;9:1505–20. https://doi.org/10.1163/156856195X00158.

[59] Beehag A, Ye L. Fibre/Matrix adhesion in thermoplastic composites : is transcrystallinity a key? Proc ICCM-11 1997.

[60] Folkes MJ, Kalay G, Ankara A. The effect of heat treatment on the properties of PEEK and APC2. Compos Sci Technol 1993;46:77–83. https://doi.org/10.1016/0266-3538(93)90083-S.

[61] Saiello S, Kenny J, Nicolais L. Interface morphology of carbon fibre/PEEK composites. J Mater Sci 1990;25:3493–6. https://doi.org/10.1007/BF00575375.

[62] Kwei TK, Schonhorn H, Frisch HL. Dynamic mechanical properties of the transcrystalline regions in two polyolefins. J Appl Phys 1967;38:2512–6. https://doi.org/10.1063/1.1709938.

[63] Matsuoka S, Daane JH, Bair HE, Kwei TK. A further study of the properties of transcrystalline regions in polyethylene. J Polym Sci [B] 1968;6:87–91. https://doi.org/10.1002/pol.1968.110060117.

[64] Zhang M, Xu J, Zhang Z, Zeng H, Xiong X. Effect of transcrystallinity on tensile behaviour of discontinuous carbon fibre reinforced semicrystalline thermoplastic composites. Polymer 1996;37:5151–8. https://doi.org/10.1016/0032-3861(96)00341-2.

[65] Choupin T, Debertrand L, Fayolle B, Régnier G, Paris C, Cinquin J, et al. Influence of thermal history on the mechanical properties of poly(ether ketone ketone) copolymers. Polym Cryst 2019;2:e10086. https://doi.org/10.1002/pcr2.10086.

[66] Kobayashi H, Hayakawa E, Kikutani T, Takaku A. Effect of quenching and annealing on fiber pull-out from crystalline polymer matrices. Adv Compos Mater 1991;1:155–68. https://doi.org/10.1163/156855191X00252.

[67] Beehag A, Ye L. Influence of cooling rate on interlaminar fracture properties of unidirectional commingled CF/PEEK composites. Appl Compos Mater 1995;2:135–51. https://doi.org/10.1007/BF00567748.

[68] Beehag A, Ye L. Role of cooling pressure on interlaminar fracture properties of commingled CF/PEEK composites. Compos Part Appl Sci Manuf 1996;27:175–82. https://doi.org/10.1016/1359-835X(95)00027-Y.

[69] Weiss R. Influence of production parameters on the mechanical behaviour of CF/PEEK. Dev. Sci. Technol. Compos. Mater., Stuttgart: 1990, p. 1007–12.

[70] Comer AJ, Ray D, Obande WO, Jones D, Lyons J, Rosca I, et al. Mechanical characterisation of carbon fibre–PEEK manufactured by laser-assisted automated-tape-placement and autoclave. Compos Part Appl Sci Manuf 2015;69:10–20. https://doi.org/10.1016/j.compositesa.2014.10.003.

[71] Avrami M. Kinetics of phase change. I: General theory. J Chem Phys 1939;7:1103–12. https://doi.org/10.1063/1.1750380.

[72] Chelaghma SA, De Almeida O, Margueres P, Passieux J, Perie J, Vinet A, et al. Identification of isothermal crystallization kinetics of poly(ether-ketone-ketone) based on spherulite growth measurements and enthalpic data. Polym Cryst 2020;3. https://doi.org/10.1002/pcr2.10141.

[73] Banks W, Sharples A, Hay JN. The effect of simultaneously occurring processes on the course of polymer crystallization. J Polym Sci A 1964;2:4059–67. https://doi.org/10.1002/pol.1964.100020923.

[74] Cowie JMG. The crystalline state: Kinetics of crystallization. Polym. Chem. Phys. Mod. Mater. 2nd edition, Blackie Academic & Professional; 1998.

[75] Hoffman JD, Lauritzen JI. Crystallization of bulk polymers with chain folding: theory of growth of lamellar spherulites. J Res Natl Bur Stand Sect Phys Chem 1961;65A:297–336. https://doi.org/10.6028/jres.065a.035.

[76] Nakamura K, Katayama K, Amano T. Some aspects of nonisothermal crystallization of polymers. II. Consideration of the isokinetic condition. J Appl Polym Sci 1973;17:1031–41. https://doi.org/10.1002/app.1973.070170404.

[77] Ziabicki A. Theoretical analysis of oriented and non isothermal crystallization. Colloid Polym Sci 1974;252:207–21.

[78] Patel RM, Spruiell JE. Crystallization kinetics during polymer processing—Analysis of available approaches for process modeling. Polym Eng Sci 1991;31:730–8. https://doi.org/10.1002/pen.760311008.

[79] Ozawa T. Kinetics of non-isothermal crystallization. Polymer 1971;12:150–8. https://doi.org/10.1016/0032-3861(71)90041-3.

[80] Bianchi O, Oliveira RVB, Fiorio R, Martins JDN, Zattera AJ, Canto LB. Assessment of Avrami, Ozawa and Avrami–Ozawa equations for determination of EVA crosslinking kinetics from DSC measurements. Polym Test 2008;27:722–9. https://doi.org/10.1016/j.polymertesting.2008.05.003.

[81] Di Lorenzo ML, Silvestre C. Non-isothermal crystallization of polymers. Prog Polym Sci 1999;24:917–50. https://doi.org/10.1016/S0079-6700(99)00019-2.

[82] Long Y, Shanks RA, Stachurski ZH. Kinetics of polymer crystallisation. Prog Polym Sci 1995;20:651–701. https://doi.org/10.1016/0079-6700(95)00002-W.

[83] Tierney JJ, Gillespie JW. Crystallization kinetics behavior of PEEK based composites exposed to high heating and cooling rates. Compos Part Appl Sci Manuf 2004;35:547–58. https://doi.org/10.1016/j.compositesa.2003.12.004.

[84] Tobin MC. Theory of phase transition kinetics with growth site impingement. I. Homogeneous nucleation. J Polym Sci Polym Phys Ed 1974;12:399–406. https://doi.org/10.1002/pol.1974.180120212.

[85] Tobin MC. The theory of phase transition kinetics with growth site impingement. II. Heterogeneous nucleation. J Polym Sci Polym Phys Ed 1976;14:2253–7. https://doi.org/10.1002/pol.1976.180141210.

[86] Tobin MC. Theory of phase transition kinetics with growth site impingement. III. Mixed heterogeneous–homogeneous nucleation and nonintegral exponents of the time. J Polym Sci Polym Phys Ed 1977;15:2269–70. https://doi.org/10.1002/pol.1977.180151217.

[87] Choe CR, Lee KH. Nonisothermal crystallization kinetics of poly(etheretherketone) (PEEK). Polym Eng Sci 1989;29:801–5. https://doi.org/10.1002/pen.760291208.

[88] Chelaghma S, Passieux J-C, Almeida OD, Périé J-N, Marguères P, Vinet A. Modélisation Pixel Coloring de la cristallisation du PEKK. Comptes Rendus JNC 21 - Bordx INP 2019:9.

[89] Ruan C, Ouyang J, Liu S, Zhang L. Computer modeling of isothermal crystallization in short fiber reinforced composites. Comput Chem Eng 2011;35:2306–17. https://doi.org/10.1016/j.compchemeng.2010.11.011.

[90] Ruan C, Guo L, Liang K, Li W. Computer modeling and simulation for 3D crystallization of polymers. II. Non-isothermal case. Polym-Plast Technol Eng 2012;51:816–22. https://doi.org/10.1080/03602559.2012.671413.

[91] Ruan C, Liang K, Guo L, Li W. Computer modeling and simulation for 3D crystallization of polymers. I. Isothermal case. Polym-Plast Technol Eng 2012;51:810–5. https://doi.org/10.1080/03602559.2012.671412.

[92] Guan X, Pitchumani R. Modeling of spherulitic crystallization in thermoplastic tow-placement process: Spherulitic microstructure evolution. Compos Sci Technol 2004;64:1363–74. https://doi.org/10.1016/j.compscitech.2003.10.023.

[93] Guan X, Pitchumani R. Modeling of spherulitic crystallization in thermoplastic tow-placement process: heat transfer analysis. Compos Sci Technol 2004;64:1123–34. https://doi.org/10.1016/j.compscitech.2003.08.011.

[94] Hosseini SMA, Schäkel M, Baran I, Janssen H, van Drongelen M, Akkerman R. Non-uniform crystallinity and temperature distribution during adjacent laser-assisted tape winding process of carbon/PA12 pipes. Int J Adv Manuf Technol 2020;111:3063–82. https://doi.org/10.1007/s00170-020-06215-8.

[95] Flanagan M, Goggins J, Doyle A, Weafer B, Ward M, Bizeul M, et al. Out-of-autoclave manufacturing of a stiffened thermoplastic carbon fibre PEEK panel. AIP Conf Proc 2017;1896. https://doi.org/10.1063/1.5008001.

[96]   Gruber MB, Lockwood IZ, Dolan TL, Funck SB, Tierney JJ, Simacek P, et al. Thermoplastic in situ placement requires better impregnated tapes and tows. Int SAMPE Tech Conf 2012.

[97]   Lamontia M, Gruber M. Remaining developments required for commercializing in situ thermoplastic ATP. SAMPE Eur Conf 2007:1–15.

[98]   Qureshi Z, Swait T, Scaife R, El-Dessouky HM. In situ consolidation of thermoplastic prepreg tape using automated tape placement technology: potential and possibilities. Compos Part B Eng 2014;66:255–67. https://doi.org/10.1016/j.compositesb.2014.05.025.

[99]   Shadmehri F, Hoa SV, Fortin-Simpson J, Ghayoor H. Effect of in situ treatment on the quality of flat thermoplastic composite plates made by automated fiber placement (AFP). Adv Manuf Polym Compos Sci 2018;4:41–7. https://doi.org/10.1080/20550340.2018.1444535.

[100] Kishore V, Ajinjeru C, Duty C. Rheological characteristics of fiber reinforced poly(ether ketone ketone) (PEKK) for melt extrusion additive manufacturing, 2017, p. 9.

[101] Cheng K, Liu Y, Wang R, Zhang J, Jiang X, Dong X, et al. Topological optimization of 3D printed bone analog with PEKK for surgical mandibular reconstruction. J Mech Behav Biomed Mater 2020;107:103758. https://doi.org/10.1016/j.jmbbm.2020.103758.

[102] Wang M, Bhardwaj G, Webster T. Antibacterial properties of PEKK for orthopedic applications. Int J Nanomedicine 2017;Volume 12:6471–6. https://doi.org/10.2147/IJN.S134983.

[103] Panayotov IV, Orti V, Cuisinier F, Yachouh J. Polyetheretherketone (PEEK) for medical applications. J Mater Sci Mater Med 2016;27:118. https://doi.org/10.1007/s10856-016-5731-4.

[104] Yang C, Tian X, Li D, Cao Y, Zhao F, Shi C. Influence of thermal processing conditions in 3D printing on the crystallinity and mechanical properties of PEEK material. J Mater Process Technol 2017;248:1–7. https://doi.org/10.1016/j.jmatprotec.2017.04.027.

[105] Yi N, Davies R, Chaplin A, McCutchion P, Ghita O. Slow and fast crystallising poly aryl ether ketones (PAEKs) in 3D printing: Crystallisation kinetics, morphology, and mechanical properties. Addit Manuf 2021;39:101843. https://doi.org/10.1016/j.addma.2021.101843.

[106] Nachtane M, Tarfaoui M, Ledoux Y, Khammassi S, Leneveu E, Pelleter J. Experimental investigation on the dynamic behavior of 3D printed CF-PEKK composite under cyclic uniaxial compression. Compos Struct 2020;247:112474. https://doi.org/10.1016/j.compstruct.2020.112474.